

Geochemistry of the Tasiussarsuaq 'greenstone-granite' terrane, southern West Greenland

Mineral resource assessment of the
Archaean Craton (66° to 63°30'N)
SW Greenland Contribution no. 10

Anders Scherstén & Henrik Stendal



GEOLOGICAL SURVEY OF DENMARK AND GREENLAND
MINISTRY OF CLIMATE AND ENERGY

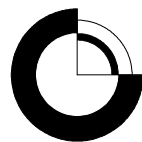


G E U S

Geochemistry of the Tasiussarsuaq 'greenstone-granite' terrane, southern West Greenland

Mineral resource assessment of the
Archaean Craton (66° to 63°30'N)
SW Greenland Contribution no. 10

Anders Scherstén & Henrik Stendal



Introduction.....	2
Background	4
Samples and methods.....	4
Qooqut Lake (Færingsehavn terrane)	4
Analytical results	5
Tasiuarsuaq terrane	11
Area 1.....	13
Detail area 2	14
Detail area 3 - Nunatak 1390.....	15
Reconnaissance areas.....	17
Analytical results	19
Melanocratic to ultramafic rocks	19
Felsic rocks.....	27
Discussion.....	30
Melanocratic to ultramafic rocks	30
Summary	35
Acknowledgements	36
References.....	37

Introduction

During the field campaigns in the Nuuk region (2004,-2007) one of the objectives was to describe Archaean primary geological environments (Hollis *et al.* 2006). This study is carried out in the northern part of the Tasiussarsuaq terrane (Fig. 1). Well preserved volcanic successions are interpreted as a former ocean floor environment that is overlain and intruded by volcanic arc rocks. The rocks comprise volcanic sequences of melanocratic- to ultramafic rocks, leucocratic volcanic rocks and granites, which were metamorphosed at upper greenschist to granulite facies conditions.

Available published maps from the region are GEUS/GGU 1:500 000 Frederikshåb Isblink - Søndre Strømfjord geological map sheet (Allaart 1982), four 1:100 000 map sheets (Qorqut 64 V.1 Syd (McGregor 1984), Buksefjorden 63 V.1 Nord (Chadwick & Coe 1983), Kangiat Nuna 63 V2 Nord (Escher 1981), and an unpublished sketch of the Kapisillit map sheet formed the basis for this work. Further descriptions and references of the involved areas can be found in Appel *et al.* (2003, 2005), Chadwick & Coe (1983), Eilu *et al.* (2006), Garde (1997), Hollis *et al.* (2004, 2006), Hollis (2005), McGregor (1993), Nielsen *et al.* (2004), Stensgaard *et al.* (2006), Stendal (2007) and Stendal and Scherstén (2007a; 2007b).

The aim of the project is to improve the understanding of the relationships and evolution of melanocratic rocks (greenstone belts) with respect to their genesis and their mineral potential, especially precious metals. The field work focused on the area southeast of Kangerdluarssengup taserssua and one area around Qooqqut lake (Fig. 1). The reason to include the Qooqqut Lake area was to deduce if the pillow sequence (Hollis *et al.* 2006) was similar to the rocks from the Tasiussarsuaq terrane. The investigations comprised geological mapping of selected areas and investigations of hydrothermal alterations for possible gold-bearing rocks. The detailed studies included melanocratic- to ultramafic sequences and granitoids in the Tasiussarsuaq terrane. Sampling of representative lithological units and mineralised rocks was carried out and the rocks have been analysed for major and trace elements.

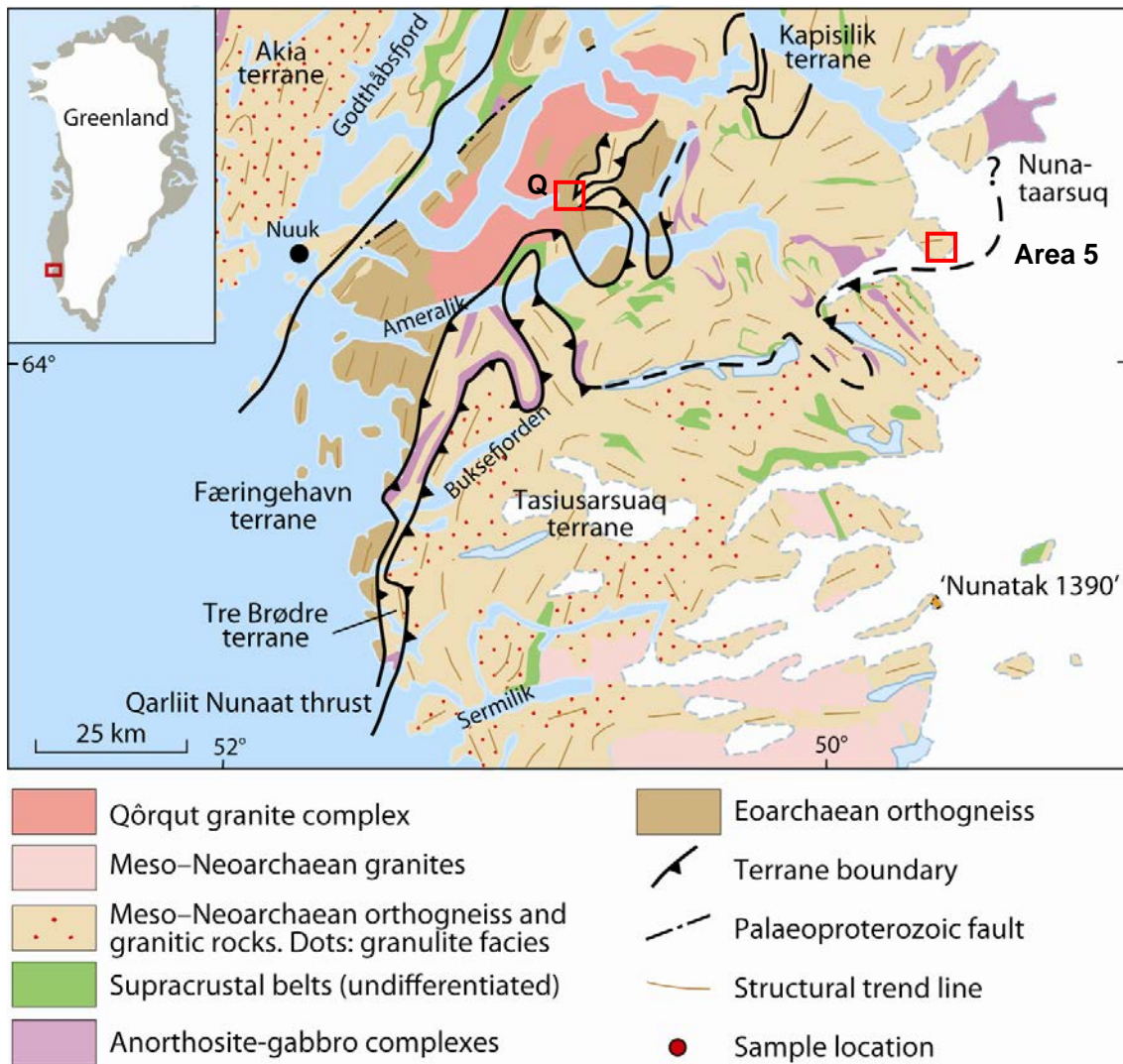


Figure 1. Geological map of the Nuuk region and location of the Nunatak 1390 study area modified after Escher & Pulvertaft (1995). The northern Tasiussarsuaq terrane boundary is outlined with solid and stippled line, but very uncertain to the east. Kangerdluarssengup taserssua is the East-West trending lake that approximate the northern Tasiussarsuaq terrane boundary. Qooquut Lake (Q) and reconnaissance area 5 are marked with red squares and lies outside the Tasiussarsuaq terrane although are has been included as it might in fact belong to the Tasiussarsuaq terrane (c.f. Windley & Garde, submitted).

Background

From 2004 to 2007 GEUS has investigated various aspects of the geology of supracrustal belts in the Nuuk region, in particular focussing on understanding aspects of the primary geological environments and their mineral occurrences, geological setting, and alteration patterns. Detailed mapping of key areas in 2004, 2005, 2006 and 2007 and targeted geochemistry and geochronology has identified Mesoarchaean greenstone belts.

Understanding the primary greenstone-granite environment of these supracrustal rocks and the alteration patterns is important in relation to understand the formation of mineral occurrences. However, it is complicated by 1) the rarity of preserved primary structures due to hydrothermal alteration, metamorphism, and multiple deformation events; and 2) the recognition of tectonic imbrications probably of rocks of widely different ages, and which might be formed in different geological environments. To solve some of these difficulties, field work was carried out in different key areas. This project is co-financed between the Greenland Bureau of Mines and Petroleum (BMP) and GEUS.

Samples and methods

87 melanocratic to ultramafic rocks and 18 granites and felsic gneisses and extrusive rocks were analysed for major and trace element abundances at Actlabs Canada. 26 of these are from the Qooqut Lake, for which major element analyses are lacking.

Qooqut Lake (Færingehavn terrane)

The Qooqut Lake area (Figs. 1, 2) was investigated due to its predicted gold potential by Nielsen *et al.* (2004). The geology is shortly described in Hollis *et al.* (2006) and the area probably belongs to the Færingehavn terrane. The quartzo-feldspathic gneisses of the area have been strongly deformed, migmatised and intruded by Ikkattoq gneisses and granite veins of the Qôrquq granite complex. Younger supracrustal rocks are intercalated with the Amitsoq gneisses and intruded by the Ikkattoq gneisses. The melanocratic supracrustal sequence is up 100 m wide and comprises abundant amphibolites and minor exhalites (quartz-garnet rocks), metasediments (rusty garnet-bearing layers) intercalated with layered melanocratic, and ultramafic rocks. Both the ultramafic rocks and the amphibolites have magnetite-bearing markers, which occur as dm–m wide layers within the rock units. The rock associations also carry minor bodies of textured metagabbros and metadolerites. A pillowd melanocratic volcanic sequence was recorded at the southern end of the Lake Qooqut, in a place where melanocratic rocks do not appear on the 1:100.000 scale geological map (McGregor 1993). The amphibolites and exhalite layers have varying amounts of sulphides, most commonly pyrrhotite with minor chalcopyrite. The amphibolites are bleached and calc-silicate altered, commonly in the vicinity of the rusty metasediments (exhalites).

Analytical results

The sample list and analytical results from the Qooqqut area are listed in Appendix I. One exhalite within the amphibolites is Cu, Ni and Zn-bearing (499013–016) with maximum values 0.13%, 0.17% and 0.4%, respectively. The highest Ni values are found in ultramafic rocks (up to 0.3%), which also have high Cr (up to 0.58%) and high Mg (up to 23%). Other exhalite bands are mainly Cu-bearing (Table 2) with up to 0.61% (e.g. 499002–003 and 499031–034). The precious metal values are low except for one sample (499014) with elevated Pt (26 ppb). Gold is not detected in the analysed samples. Further work by Steensgaard *et al.* (2006) did not add any further precious metal anomalies either in rocks or stream sediment samples.

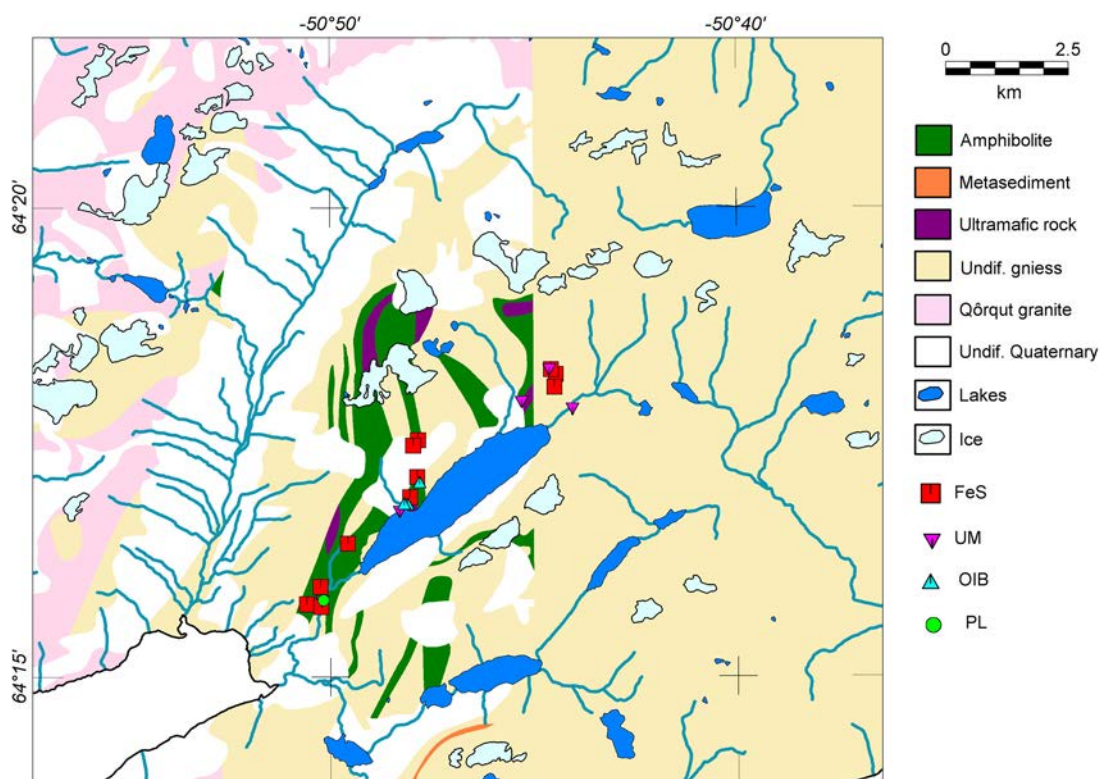


Figure 2. Map of the Qooqqut Lake area (central elongate NE-trending lake). The north-south trending “fault line” is a map artefact from lacking information to the east.

Major elements have not been analysed for the Qooqqut Lake rocks, which prohibits a comprehensive interpretation of these rocks. Trace elements show substantial scatter, in part due to the sample selection, which includes a number of altered and mineralised samples. Three of the Qooqqut Lake rocks are atypical for SW Greenland greenstones. These amphibolites have enriched and smooth mantle normalised incompatible trace element abundances (Fig. 3) and $\Delta\text{Nb}=0.33-0.39$ (Fitton *et al.*, 1997); a signature that is typical for ocean island basalts (OIB). It is argued that ΔNb is robust against melting and crustal contamination effects (Fitton *et al.*, 1997), which might imply that these anomalies are not secondary. Nevertheless, these high Nb concentrations are associated with V enrichment, and the Nb-anomalies could also be due to magnetite fractionation, which is noted in these rocks (Fig. 3). However, the remaining samples are also magnetite bearing,

have similar V-concentrations and show no evidence of Nb enrichment associated with high V (Fig. 4). Furthermore, magnetite fractionation would not have any effect on the rare earth element (REE) patterns, and the unique signature of these three samples is difficult to reconcile with contamination or fractionation processes.

High $Gd/Yb_N=3.9\text{--}4.3$ likely reflects a garnet residue from the melting. At face value, $Nb/Th > 10$ requires a moderately depleted mantle source (i.e. more depleted than primitive mantle; Fig. 5). Nb/Th is sensitive to continental crust contamination, which decreases the ratio, but there are no signs of such processes. It thus seems as if there is a unique component in this sample set, which seems to require an OIB-like source.

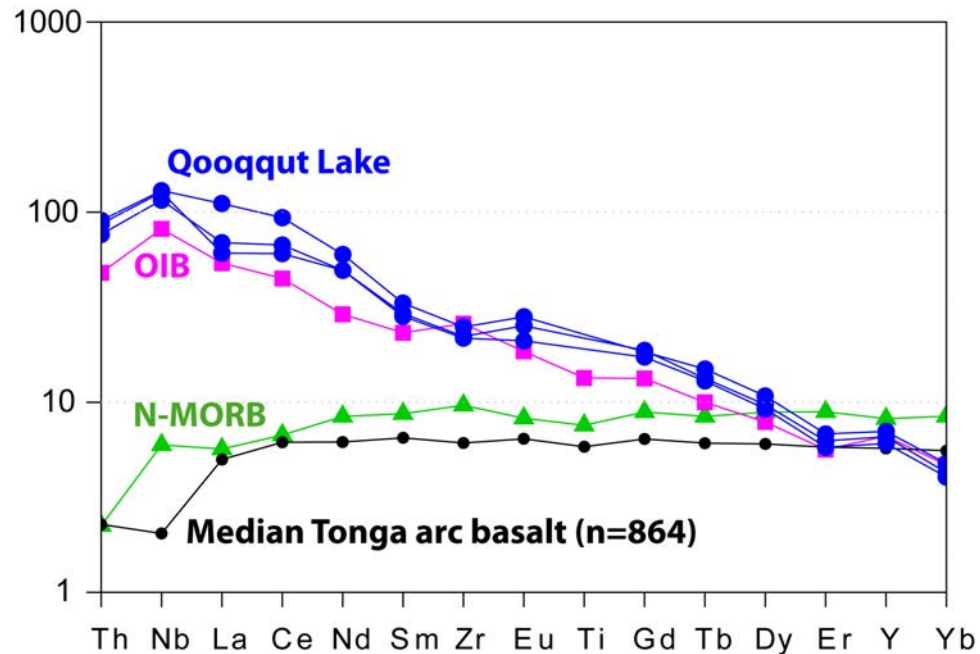


Figure 3. Primitive mantle normalised (Palme & O'Neill, 2003) trace element diagram for the enriched Qooqqu Lake amphibolites, which have an OIB-like signature. Reference data for OIB is from Sun & McDonough (1989), N-MORB is from Hofmann (1988) and Tonga arc basalts are from GEOROC (<http://georoc.mpch-mainz.gwdg.de/Entry.html>). OIB denotes Ocean Island Basalt and N-MORB Normal Mid-Ocean Ridge Basalt.

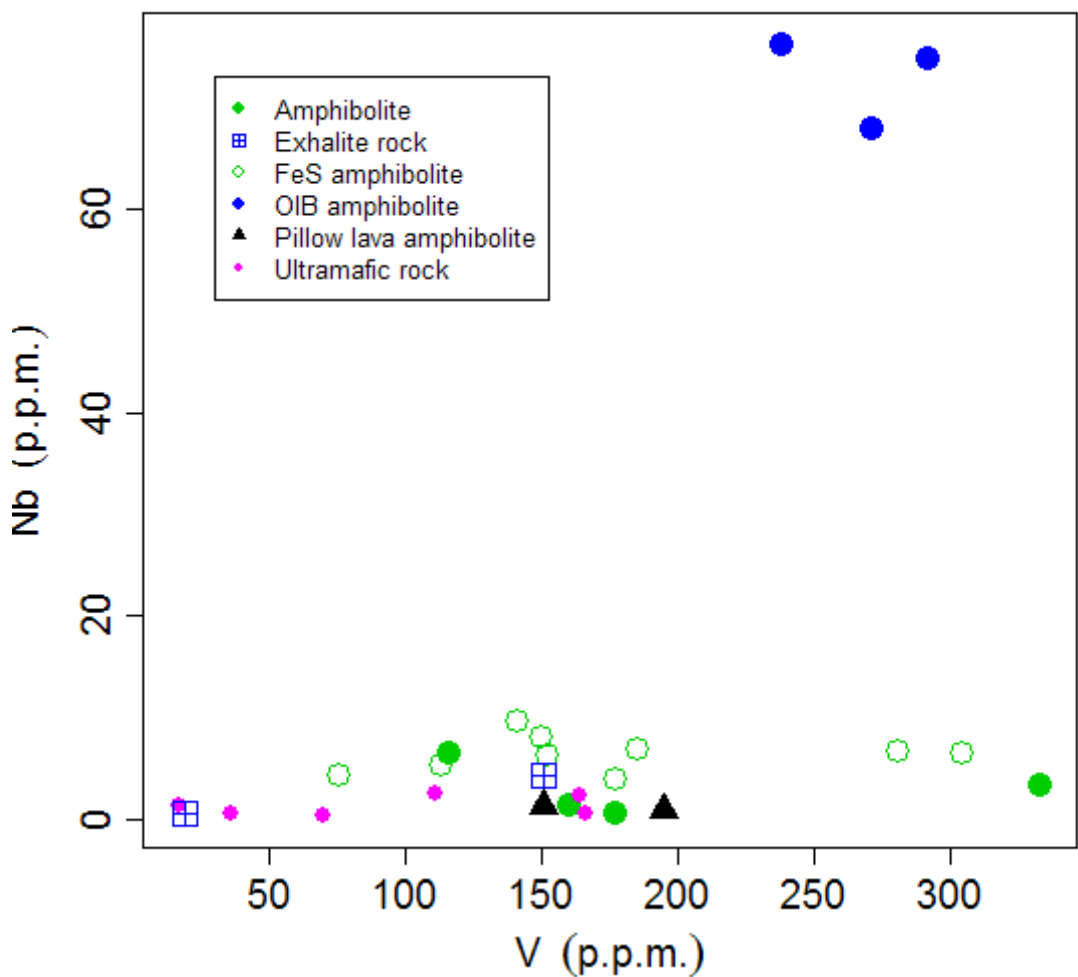


Figure 4. V plotted against Nb for amphibolites (filled green circles), iron sulphide bearing amphibolites (open green circles) OIB-like amphibolites (filled blue circles), amphibolites with pillow lava structures (black triangles) and ultramafic rocks (filled purple circles). The OIB-like amphibolites have strongly enriched Nb , and V , although their V -concentrations are within the range of the other amphibolites.

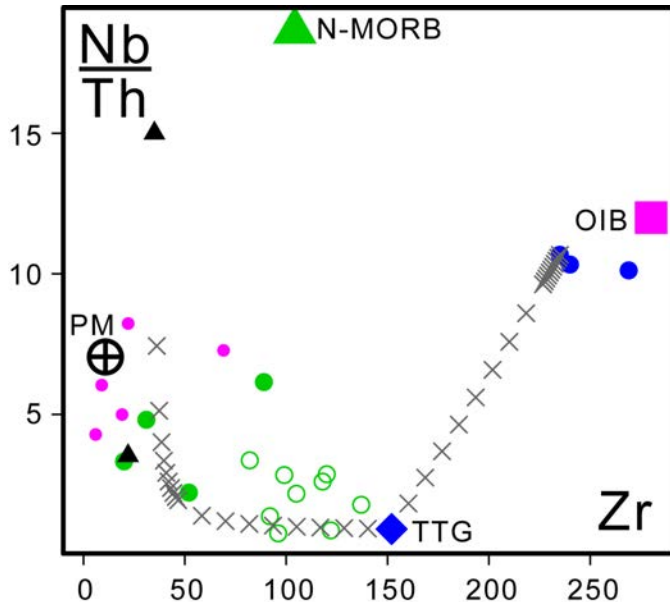


Figure 5. Zr (ppm) and Nb/U plotted against Nb/Th for the Qooqut Lake samples. See figure 4 for sample legend. PM: Primitive Mantle, OIB: Ocean Island Basalt, N-MORB: Normal Mid-Ocean Ridge Basalt and TTG: Tonalite-Trondhjemite-Granodiorite gneisses. Mixing curves between TTG and OIB-like or N-MORB like end-members are indicated with an x for each 10% mixing increment, except for the first ten at the N-MORB or OIB end, which denote 1% mixing increments.

The remaining samples are characterised by negative Nb-anomalies and Nb/Th and Nb/La values that are lower than primitive mantle (Fig. 6). REE are variable with $La/Yb_N=0.5-12.5$ and concentrations ranging from sub-chondritic to nearly 100 times chondrite (Fig. 6). This large span is broadly correlated with a shift from negative Eu-anomalies for the samples with the lowest abundances to positive anomalies for the samples with the highest abundances (Fig. 6). The shift is likely reflecting igneous fractionation and plagioclase removal or addition in the evolving magmas.

Two samples from a pillow lava section were analysed. One contains calc-silicate lenses and one is relatively pure amphibolite. The latter differs from the majority of the amphibolites from the area and is characterised by MORB-like trace element ratios, but with lower concentrations (Fig. 6). The calc-silicate bearing sample, is slightly more enriched in the most incompatible elements, and has a significant negative Nb-anomaly (Fig. 6). It is unlikely that the Nb-anomaly stems from alteration, but might be a continental crust signature, either through sediment input or by contamination during emplacement. Figure 7 outlines the effect of crustal contamination of a MORB-like end-member, which we assume is represented by the pillow structure amphibolite. The calc-silicate pillow structure amphibolite makes a moderately good fit with a few percent crustal contamination, although decreasing Sm/Zr with increasing degrees of contamination is not observed. Likewise, a positive Eu-anomaly in the pillowed structure amphibolite might represent unaccounted assimilation fractional crystallisation (AFC) processes such as plagioclase cumulation prior to eruption.

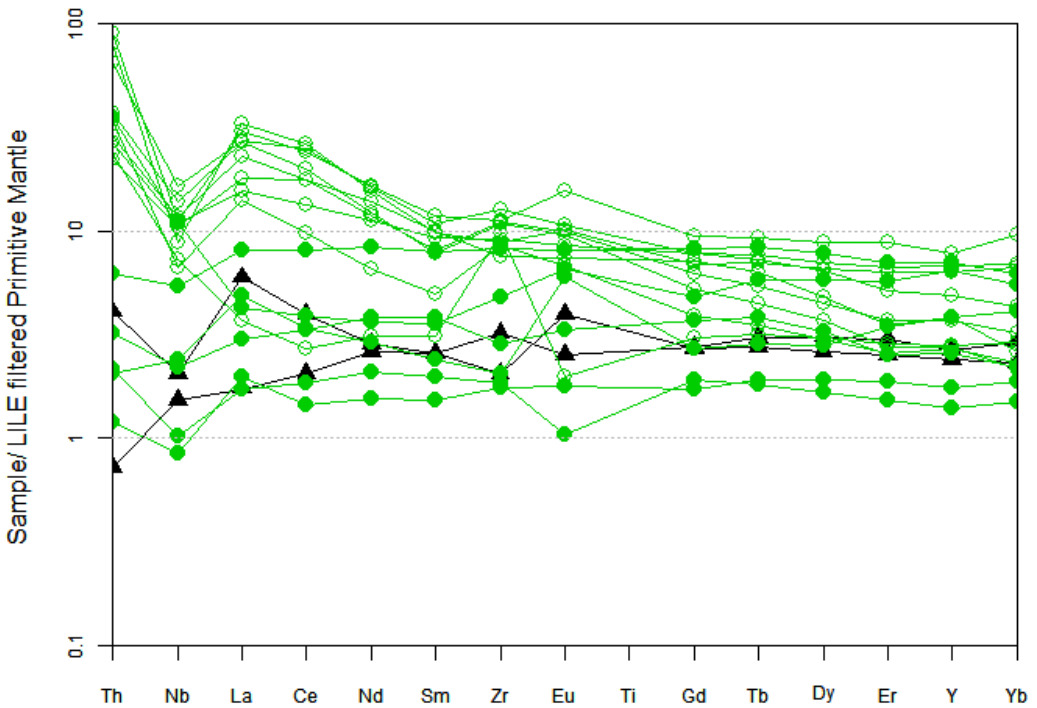


Figure 6. Primitive mantle normalised (Palme & O'Neill, 2003) trace element diagram for Qooqut Lake amphibolites and FeS-mineralised amphibolites. The FeS-mineralised amphibolites are generally more enriched in incompatible trace elements than the barren amphibolites, and display lower Nb/Th. Legend as in Fig. 4.

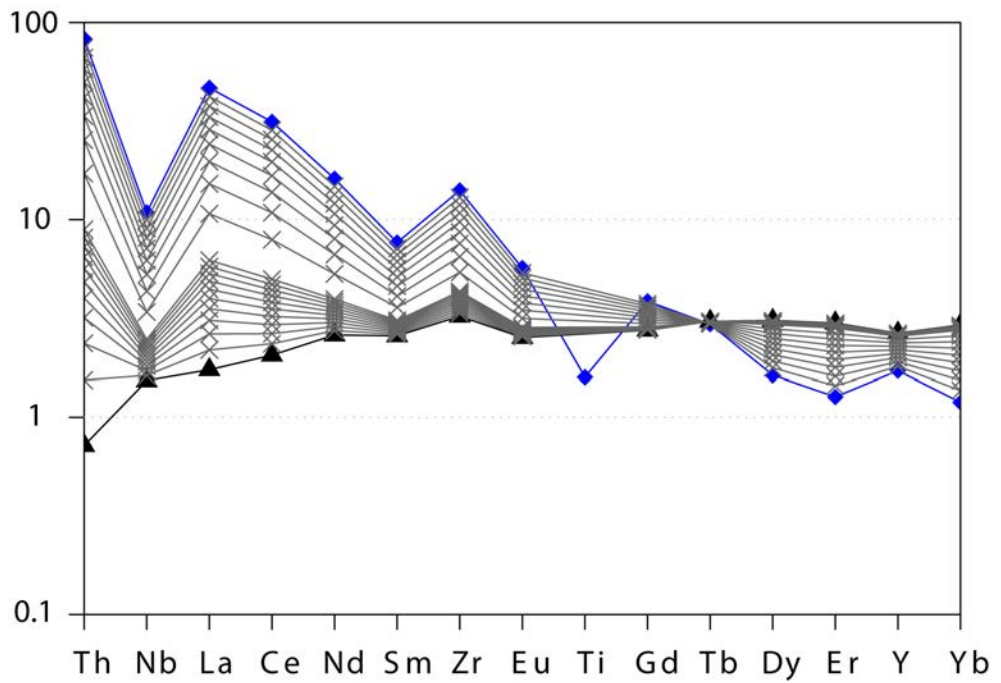


Figure 7. Primitive mantle normalised (Palme & O'Neill, 2003) trace element diagram for the MORB like pillow lava amphibolite (black triangles) and average Archaean TTG (blue diamonds, data from Kemp & Hawkesworth, 2003) and mixed compositions between these two end-members. The first ten curves from the MORB-like end-member represents 1% mixing increments, while the remaining are 10% increments.

The amphibolite samples were divided into two subsets, FeS-mineralised (mainly iron sulphides), and non-mineralised. The FeS-mineralised amphibolites are strikingly different from the pillow structure amphibolites in that they are more enriched in the most incompatible elements and with pronounced negative Nb-anomalies (Fig. 6). The cause of the enrichment might be complex, but here we will consider crustal contamination, alteration with or without mass changes or mantle source enrichment. AFC processes where crustal contamination plays a significant part might explain the array. Mixing with the OIB-like components represented by three samples is, however, untenable (Fig. 5). Alteration with associated mass changes can increase or decrease the immobile element concentrations, but is not expected to shift their ratios; for instance Nb/Th. The variation in Nb/Th is greater in the non mineralised samples, while Zr concentrations are primarily variable in the FeS-mineralised amphibolites. It is conceivable that the variation in Nb/Th is related to crustal contamination, while the mineralisation processes were associated with alteration that caused mass changes and increased Zr concentrations in the FeS-mineralised samples, but small changes in Nb/Th (Fig. 5).

The ultramafic rocks are not shown in figures 4 & 5 as their element concentrations are too close to the detection limits, and these data do not allow meaningful interpretations.

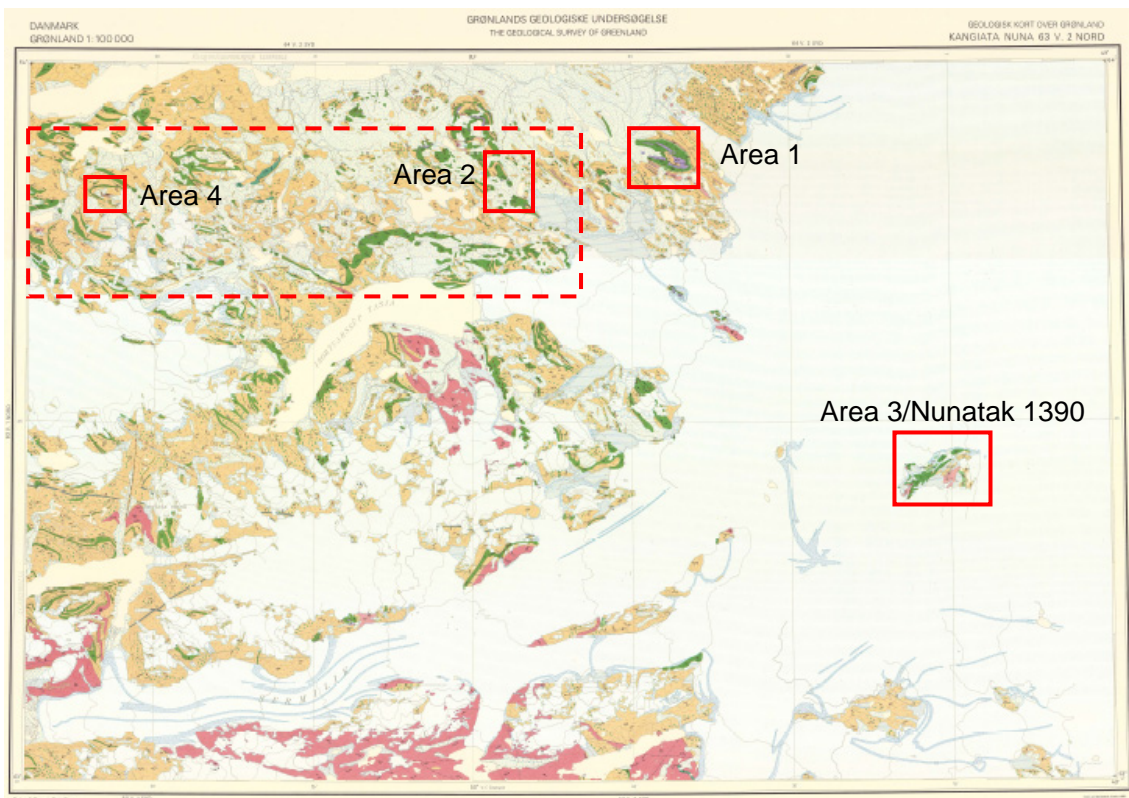
Tasiuarsuaq terrane

The Tasiuarsuaq terrane (e.g. Friend & Nutman 2001, 2005; Hollis *et al.* 2006; Stendal 2007; Stendal & Scherstén 2007a, b; Kolb & Stendal 2007; Næraa & Scherstén, 2008) southeast of Kangerdluarssenguup taserssua is dominated by tonalitic to granodioritic gneisses, the deformed Ilivertalik augen granite and melanocratic to ultramafic rocks (Fig. 8). The melanocratic to ultramafic rocks include amphibolites with calc-silicate alteration and sometimes preserved pillow lavas, massive amphibolite (occasionally with gabbroic textures), and ultramafic pods and dykes, sometimes associated with magnetite-bearing, black amphibolite. Dimensions of these melanocratic to ultramafic complexes ranges from 50 up to more than 1000 m, and they are intruded by granitoid gneisses and cross-cut by brown-weathered dolerite dykes (up to 30 m wide) with well developed chilled margins and generally strike E-W. Alteration is common within the amphibolites such as calc-silicate formation within pillow lava sequences. The pillow lava sequences have intercalations of 1 – 2 m wide rusty, sulphide-bearing layers, which are interpreted as exhalites. Occurrences of garnet-sillimanite-biotite-sulphide rocks are relatively common and likely formed by alteration processes and later metamorphism. Hydrothermal alteration likely took place in the volcanic environment.

The age of the Tasiuarsuaq terrane is assumed to be within the range of 2.92–2.84 Ga (Schiøtte *et al.*, 1989; Friend & Nutman 2001; Crowley, 2002; Næraa & Scherstén, 2008). Investigated melanocratic-ultramafic complexes are dominated by amphibolite to upper amphibolite facies metamorphic rocks, although greenschist facies rocks are present at Nunatak 1390 (Fig. 8). We assume that most of the greenstones in the Tasiuarsuaq terrane formed in a similar geo-tectonic environment.

The Kangiata Nuna 1:100.000 geological map sheet shows a large greenstone granite belt with 20 – 30% of greenstones and at least two generations of tonalite and granodiorite (Tasiuarsuaq terrane). The greenstone granite belt is estimated to make up more than 1200 km² and with possible extension towards the south. Melanocratic sequences and exhalites (greenstones) in the Tasiuarsuaq terrane south and southeast of Kangerdluarssenguup Tasersua may become economically interesting due to elevated gold and arsenic contents.

Garnet-sillimanite-biotite ±sulphide rocks seem to record a regional phenomenon. The alterations are pervasive and independent of rock types or geological terrane boundaries. The alteration must have occurred after or during the amalgamation of micro continents in the Nuuk region, but prior to regional metamorphism, if it is assumed to represent one event.



Metamorphic rocks older than 2600 m. y. in amphibolite and granulite facies

Hypersthene-bearing rocks

gi	GRANITE (<i>sensu lato</i>) intrusive, mainly tonalitic and granodioritic
Igi	ILIVERTALIK AUGEN GRANITE
gn	GNEISS, mainly tonalitic and granodioritic; foliation trends indicated <ul style="list-style-type: none"> .. with layers and fragments of amphibolite .. with fragments of anorthosite and leucogabbro .. with pods of ultramafic rocks
d	DIORITE AND TONALITE
Fy	ANORTHOSITE AND LEUCOGABBRO
a	AMPHIBOLITE of unknown origin <ul style="list-style-type: none"> .. with pods of ultramafic rocks
ae	AMPHIBOLITE of volcanic origin <ul style="list-style-type: none"> .. with pillow lava structures .. with pods of ultramafic rocks
ms	METASEDIMENT, siliceous with mica, garnet and sillimanite

Figure 8. The Kangiata Nuna map sheet 63 V2N, with the main field areas highlighted with solid red rectangles and reconnaissance areas with a stippled red rectangle.

Area 1

The detail area 1 (Figs. 1 & 8) is located 20 km NE of Isortuarssuup tasia ($63^{\circ}56.29'$ - $49^{\circ}40.62'$) and the main rock types are given in the Table 1 below. The lowest part of the sequence consists of ultramafic cumulates (>500 m) that are dominated by pyroxenites and minor harzburgites. The pyroxenites comprise coarse-grained orthopyroxene with minor fine-grained clinopyroxene, phlogopite and olivine. The melanocratic volcanic pillow sequence has some well preserved but deformed pillows, which are 5 – 50 cm large and the sequence has pronounced calc-silicate alteration with epidote, diopside and actinolite. Minor rusty layers (exhalites) occur within the pillow sequence and carry a few volume % of iron sulphides. The pillowized melanocratic rocks are overlain by gabbro and amphibolite. The gabbroic rocks are melanocratic coarse-grained volcanic flows (1 – 10 m thick) with m-thick fine-grained amphibolites (ash layers) between the flows.

Table 1. Tectonostratigraphy of area 1.

Rock type	Thickness (m)	Comment
Melanocratic dyke	1 - 30	Undeformed Palaeoproterozoic brown dykes
Alteration(rusty rocks)	5 – 50	Alteration along fault/shear zones and sulphide formation
Granitoid		Tonalite (gneiss) and granodiorite/pegmatite (two generations)
Ultramafic pillows	1 – 10	10 – 30 cm large pillows with magnetite
Ultramafic dykes	1 – 30	Feeder dykes (peridotites) for the ultramafic pillows
Melanocratic volcanic flows/ash	>200	Gabbro flows dominate but intercalated with melanocratic pillows (see below)
Melanocratic volcanic pillows	50 – 100	5 – 50 cm large pillows, pillow breccias and calc-silicate alterations
Pyroxenites/harzburgite	>500	Pyroxenites dominate

The pyroxenites/harzburgites and the melanocratic volcanic extrusions are all cut by an ultramafic dyke swarm (1 – 30 m thick) with nicely developed chilled margins. The rocks are called peridotite as a field term. These dykes are feeder dykes for ultramafic pillows (10 – 30 cm) and often have a dark chilled margin and matrix between the pillows (Fig. 9). The composition of the peridotite is dominated by olivine and coarser grained orthopyroxene.

Both the dykes and the pillows have several volume percentage of magnetite (Hollis *et al.* 2006).



Fig. 9 Ultramafic pillow structures in ultramafic rocks from Area 1.

All the melanocratic to ultramafic rocks are intruded by granitoids. Tonalitic gneiss surrounds the complex, but also appears in the centre of the melanocratic-ultramafic complex. A later intrusive rock is granodiorite that preserves intrusive relationships with the melanocratic-ultramafic complex. The granodiorite is deformed but not as much as the tonalite. Pegmatites formed contemporaneously with the granodiorite, both as irregular bodies ($\sim 10 \text{ m}^2$) and as veins.

Rust zones along fault/shear zones occur very pronounced in the middle part of the melanocratic complex. This is a biotite alteration zone where the amphibolite is altered with some Fe sulphides. One specific zone is up to 50 m wide but other rust zones are 1 – 10 m wide. The rust zones contain/are intruded by minor veins of granodiorite and pegmatite.

Detail area 2

The detail area 2 was visited in 2005 (Hollis *et al.* 2006). It was revisited because of the indication of gold and arsenic in the region. The study area contains amphibolite deduced to have originated as a pillowed melanocratic volcanic sequence. The melanocratic sequence has a similar ultramafic pillow sequence and magnetite-bearing amphibolite as observed in area 1, but the rocks here are generally more deformed and at higher metamorphic grade. The amphibolites have abundant calc-silicate minerals (diopside,

epidote and \pm garnet) and intercalations of 1 – 2 m wide rusty, sulphide-bearing layers (exhalites). The sulphides are pyrite, pyrrhotite, chalcopyrite and arsenopyrite. It is worth noting that this area is the only place outside Storø, which contains arsenic in considerable amounts. The arsenopyrite-bearing rusty amphibolite is either an exhalite or an altered amphibolite layer with some garnet formation. It was not possible to follow the mineralised layer over long distances due to coverage with mainly talus material.

The granitoids in the area comprise tonalitic gneiss and a later intrusive granodiorite. Both granite phases are intrusive into the melanocratic package. The region is crosscut by brown-weathered dykes (up to 30 m wide), which generally strikes roughly E-W and probably are Palaeoproterozoic in age.

Detail area 3 - Nunatak 1390

The detail area 3 is called ‘Nunatak 1390 m East of Alangordlia’ by Escher & Pidgeon (1976), but we will refer to it as Nunatak 1390 for simplicity. It is located 63°42.96' - 49°16.89' (Figs. 1, 8 & 10; Stendal & Scherstén 2007a, b). The main rock types are greenschist facies melanocratic and acid volcanic rocks and granitoids. The main rock units of the stratigraphy are shown in table 2 below.

Table 2. Tectonostratigraphy of area 3.

Rock type	Thickness (m)	Comments
Melanocratic dyke	1 – 20	Undeformed Palaeoproterozoic brown dykes
Granite(s)		Porphyritic granite, altered granite and pegmatite
Tuff	700 - 800	Finely laminated ash layers intruded by granitoids
Hydrothermally altered zone	50	Altered melanocratic ash – silicified and epidotised rocks
Melanocratic volcanic flows/ash	120	Basaltic-komatiitic/melanocratic-ultramafic flows and ashes, intercalated with ultramafic
Acid flows and pyroclastites	80	Acid lava flows and ignimbrites
Upper melanocratic volcanic pillows	~200	25 – 100 cm large pillows, pillow breccias and calc-silicate alterations
Ultramafic greenstone/soapstone	10 – 50	Ultramafic sill between lower and upper pillow sequence
Lower melanocratic pillow sequence	>500	Deformed pillow lavas with extensive calc-silicate alterations that are cut by melanocratic dykes

The lower melanocratic pillow sequence consists of 50 – 100 cm large deformed pillows and pillow breccias with calc-silicate alteration in the matrix between the pillows and in the centre of the pillow. The calc-silicate minerals epidote, diopside and carbonates comprise up to 20 vol% of the rock. The pillowed sequence is cut but by a slightly deformed melanocratic dyke swarm (1–5 m in thickness) striking more or less E-W. The dykes are fine- to middle-grained gabbroic or noritic rocks.

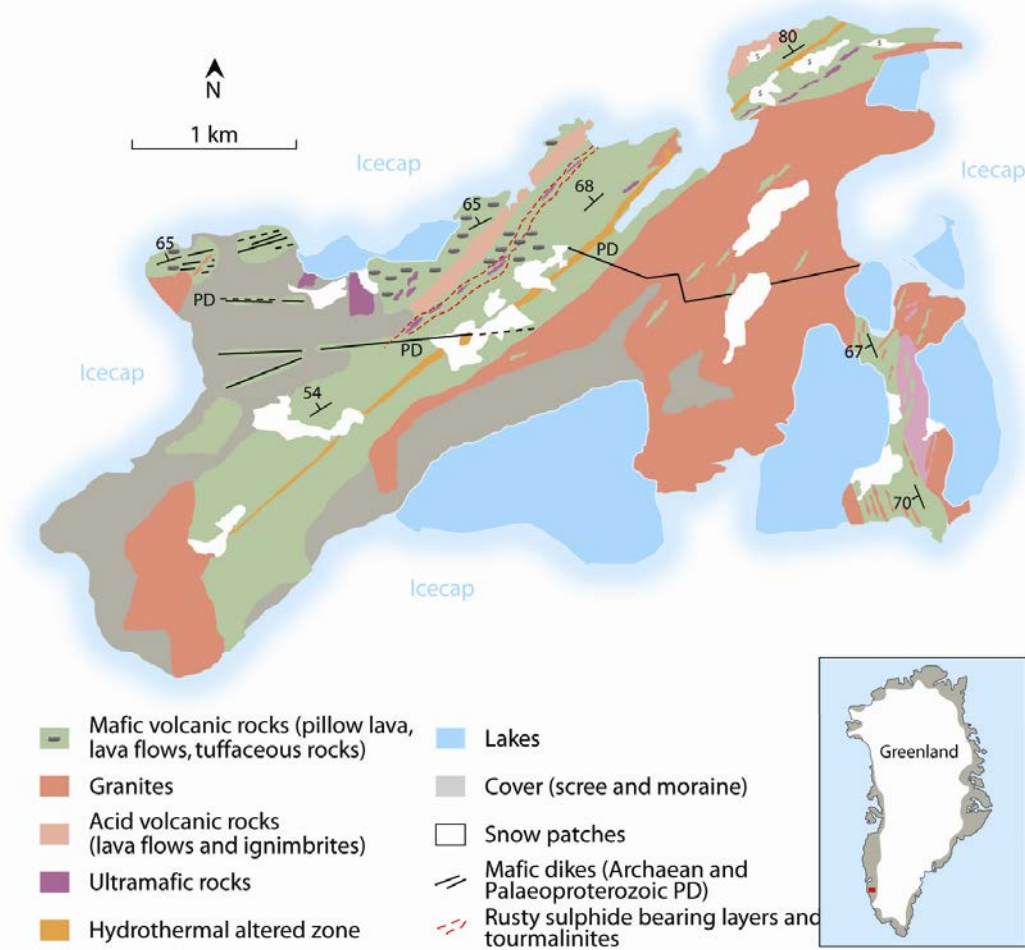


Figure 10. Map of Nunatak 1390 (modified after Stendal & Scherstén, 2007).

Ultramafic greenstones/soapstones occur between the upper and lower pillow lava sequences. These magnetite bearing greenstones/soapstones are interpreted as sills. The upper pillow sequence has very well preserved primary structures such as pillows, lava flows and ash layers. The least deformed pillow lavas and flows contain relic/preserved vesicles. Way-up criteria of the pillow structures consistently point to southeast. Interbedded in the melanocratic flows and pyroclastics is 80 m of acid volcanic rocks. The rocks are acid flows and and pyroclastic rocks (Fig. 11) and fine laminated ignimbrites. Fine-grained grey to light feldspar phenocrystic porphyritic dykes 0.3 – 0.8 m wide) cut the melanocratic and the volcanics and are interpreted as feeder dykes to the acid rocks, and Escher & Myers (1975) argue that these dykes likely intruded the pillow lavas shortly after eruption. Superimposed on the acid volcanic rocks consists of gabbroic flows and ashes with intercalation of ultramafic sills, melanocratic rusty layers with sulphides (exhalites) and

tourmalinites. The latter is an up to one metre thick layer located between the ultramafic bodies and fine laminated ash layers. The sulphides in the rusty layers are iron sulphides (e.g. pyrite) with minor chalcopyrite.



Fig. 11 Felsic volcanic rock that is interpreted as an ignimbrite at Nunatak 1390.

A prominent strike parallel hydrothermal zone consists of strongly silicified and epidotised melanocratic ash layers, which appears as hornfels. The hydrothermal altered zone is up to 50 m wide and light brownish in colour on the surface. The hydrothermal zone follows a fault lineament. The hanging wall of the hydrothermal zone comprises a thick sequence of finely laminated tuff layers. Granite intrusion abundance increases upwards in the sequence and eventually dominates with tuff xenoliths.

Two phases of granite occur, one porphyritic with K-feldspar phenocrysts up to several cm in length and nearly isotropic. The other granite phase is more even grained, medium-grained, foliated and muscovite-bearing. Parts of the granites especially in the western part are altered and have a distinct pink colouration probably due to hematite formation in the granite.

Reconnaissance areas

The mapping areas 1, 2 and 3 (Nunatak 1390) are all located on the Kangiata Nuna map sheet (Fig. 8). In addition, reconnaissance areas were mapped with the aim to investigate the amphibolites on a regional scale and to cover the map sheet. The overall impression is that a vast majority of the melanocratic to ultramafic rocks originated within the same geological environment and time period as the extrusive melanocratic volcanic rocks

described in the previous sections. Samples of amphibolite, ultramafic rocks and granitoids have been collected for geochemical comparison of the different rock types and age for determinations.

Reconnaissance camp 4 ($63^{\circ}53.82'$ and $50^{\circ}32.58'$; Fig. 8) display intrusive relationships of both tonalite and granodiorite into the melanocratic volcanic sequence. Hydrothermal alteration prior to regional amphibolite facies metamorphism caused rusty garnet-biotite, \pm sillimanite rocks \pm sulphides that occur in zones up to a couple of metres wide and continued along strike. The garnets are 1–5 mm in size and have a light pink colour (grossular?). Sulphides are common, especially in the biotite zones. The sulphides are mostly fine-grained pyrite and pyrrhotite placed in a matrix of biotite and quartz but not more than a few volume percent.

Reconnaissance camp 5 ($64^{\circ}11.39'$ - $49^{\circ}31.78'$; Fig. 1) is another area with extensive alteration of the country rock, which has recrystallised to garnet-sillimanite-biotite \pm sulphides schists during subsequent metamorphism. The area comprises presumed Amitsoq gneisses with deformed Ameralik dykes and intrusions of tonalite and granodiorite. The granitoids are foliated but clearly intrusive into the Amitsoq gneisses with discordant contacts. The garnet-sillimanite-biotite \pm sulphides schists occur in an area of approximately 1000x200 m and pervasive alteration seems to have affected all rock types but the most altered rock is grey gneiss (granodiorite) and the least altered rocks are pegmatites. The alteration occurs in many stages from faint, partly to complete alteration, which must post-date rock formation, but pre-date metamorphism. The main rock type is a garnet-sillimanite rock with up to 20 – 30 volume % of each mineral. In mylonite and shear zones biotite and Fe sulphides occurs with garnet and sillimanite and these rocks are silicified. The sulphide content does normally not exceed a few volume % of the rock. The sulphide bearing biotite shear zones are 0.5 – 1 m wide and vary in strike but a NNE-NE trend is common.

South of Ameralik

One locality was investigated in the area south of Ameralik in 2004 (Appel *et al.* 2005), where one big loose block ($\sim 1 \text{ m}^3$) was albited and disseminated with sulphides (pyrite and chalcopyrite). The analyses yield nearly 2% copper and 200 ppb gold. This area was revisited during a reconnaissance together with Bo Møller Stensgaard. The area is located in the vicinity of the transition between the Tasiussarsuaq and Tre Brødre terranes. The quartzo-feldspatic gneisses of the area have been strongly deformed, migmatised and intruded by Ikkattoq gneisses and granite veins of the Qorput granite complex. Younger supracrustal rocks are intercalated with the Amitsoq gneisses. The supracrustal rocks are amphibolite facies pillow lavas, minor bodies of metagabbros and metadolerite with minor exhalites (quartz-garnet rocks). Magnetite is abundant in these ultramafic and amphibolite rocks. The rusty layers (exhalites) have varying amounts of sulphides, most commonly pyrrhotite with minor pyrite and chalcopyrite.

Hydrothermal alteration seems to have occurred along fault/shear zones, which is now manifested by garnet-sillimanite-biotite rocks with varying amounts of iron sulphides (e.g. $64^{\circ}02.67'$ and $50^{\circ}48.75'$). The alteration zones are up to 200 m wide and all rock types (gneiss, granites, and amphibolites) are more or less altered.

Analytical results

Melanocratic to ultramafic rocks

61 rocks were analysed for major and trace elements, and all data was recalculated to 100% on a volatile free basis (appendix I). The rocks define a tholeiitic trend (Fig. 12) that range in SiO_2 between 39.7-80.0 wt% and MgO between 2.3-35.5 wt%. Compatible elements are positively correlated with MgO and range up to 3170 p.p.m. Cr and 2020 p.p.m. Ni (Fig. 13). Some of the ultramafic rocks are aluminium depleted with $\text{Al}_2\text{O}_3 < 5$ wt%. Basalt, komatiitic basalt and komatiite compositions dominate these rocks (Fig. 14)

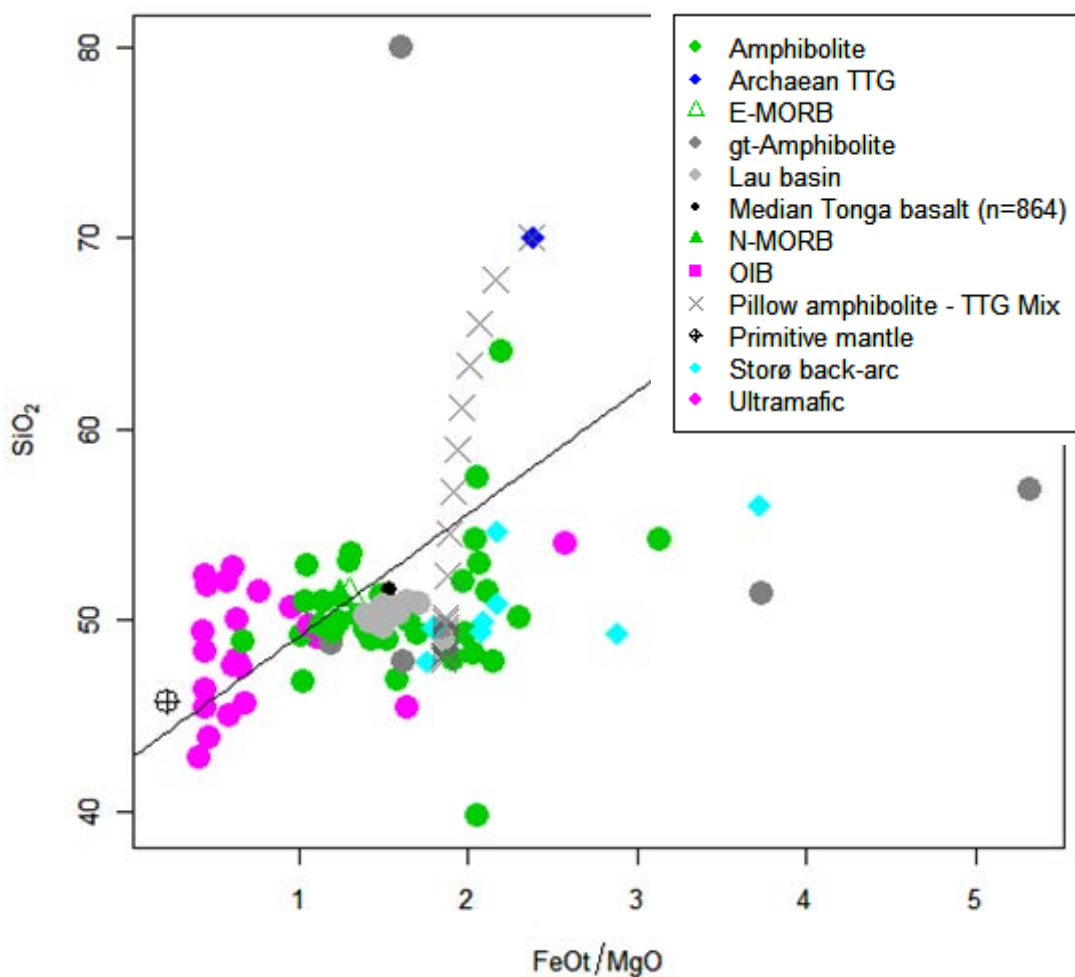


Fig. 12 The Tasiussarsuaq melanocratic amphibolites to ultramafic rocks in a FeOt/MgO versus SiO_2 diagram, where the black trend line delineates calc-alkaline trends (steeper) from tholeiitic (shallow). The Tasiussarsuaq data define a scattered tholeiitic trend. Some of the data scatter is likely due to local crustal contamination as indicated by the mixing line or by mass changes during pre-metamorphic alteration (e.g. a silicified garnet amphibolite with 80 wt% SiO_2). Data sources for Archaean TTG from Martin (1995) and Martin et al. (2005) E-MORB from Klein (2003), Lau basin from Regelous et al. (2008), Tonga basalts from GEOROC (<http://georoc.mpch-mainz.gwdg.de/georoc/>), N-MORB from Hofmann (1988), OIB from Sun and McDonough (1989) and Storø data from van Gool et al. (2008).

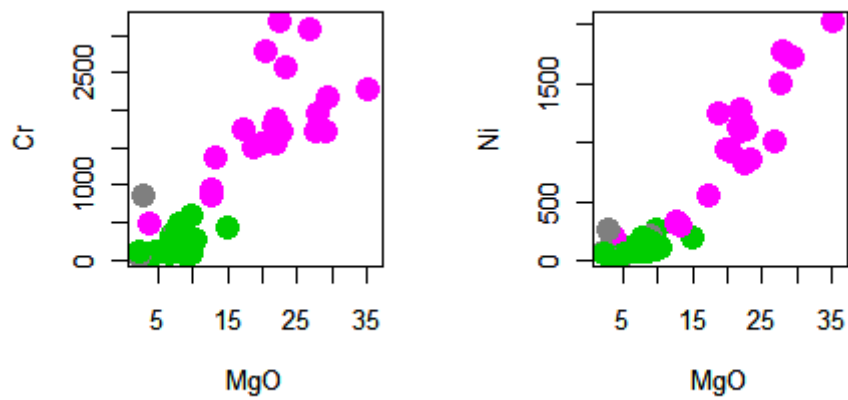


Fig. 13 *MgO variation diagrams for Cr and Ni for all Tasiussarsuaq melanocratic amphibolites and ultramafic rocks. See figure 12 for legend.*

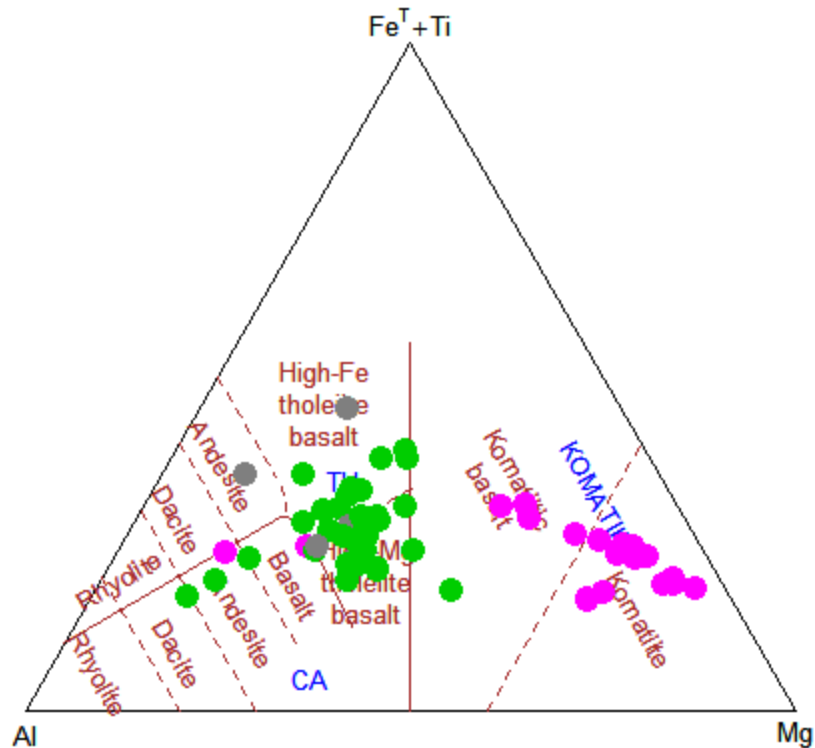


Fig. 14 *Jensen(1976) classification diagram for the melanocratic to ultramafic rocks, which are dominated by Mg-rich basaltic compositions among the amphibolites and komatiitic basalt to komatiitic compositions among the ultramafic rocks. See figure 12 for legend.*

The rocks found on Nunatak 1390 are the best preserved in this study as they preserve primary textures and serve as a reference for the remaining rocks, which are more deformed and metamorphosed. Samples from Nunatak 1390 fall into three subsets in MgO variation diagrams. One subset represents a melanocratic pillow sequence, where the samples plot within the Mg- and Fe-tholeiite basalt fields (4.5–10 wt% MgO) in a Jensen (1976) cation classification diagram. We use the Jensen diagram instead of the TAS diagram to avoid the effects of disturbed alkali element contents. The interbedded acid volcanic rocks constitute dacites (63.8–72.8 wt% SiO₂) and an andesite (55.1 wt% SiO₂) and form the second subset. The melanocratic-ultramafic sills and ash layers form the third subset and classify as komatiite, komatiitic basalt and Mg- and Fe-tholeiitic basalt. The komatiitic affinities have 16–21 wt% MgO, TiO₂ <0.65 wt% and 47.4–50.4 wt% SiO₂, and are compositionally distinct from the basalts with an SiO₂ concentration gap between 10–16 wt%. Collectively, the melanocratic-ultramafic rocks plot along a single tholeiitic trend, while the acid rocks plot along a loosely defined calc-alkaline trend.

Some of the ultramafic rocks have high Cr and Ni concentrations >1500 and >800 p.p.m. respectively. Al₂O₃ concentrations are around 15 wt%, except for some of the ultramafic rocks that have lower concentrations between 3-5 wt%. MgO ranges between 4.5-9.8 wt% in the melanocratic rocks and 16-21 wt% in the ultramafic rocks . CaO/Al₂O₃ and Al₂O₃/TiO₂ range between 0.4-1.0 and 11.0-19.9 respectively for the melanocratic rocks, and 1.75-3.15 and 5.6-8.3 respectively for the ultramafic rocks.

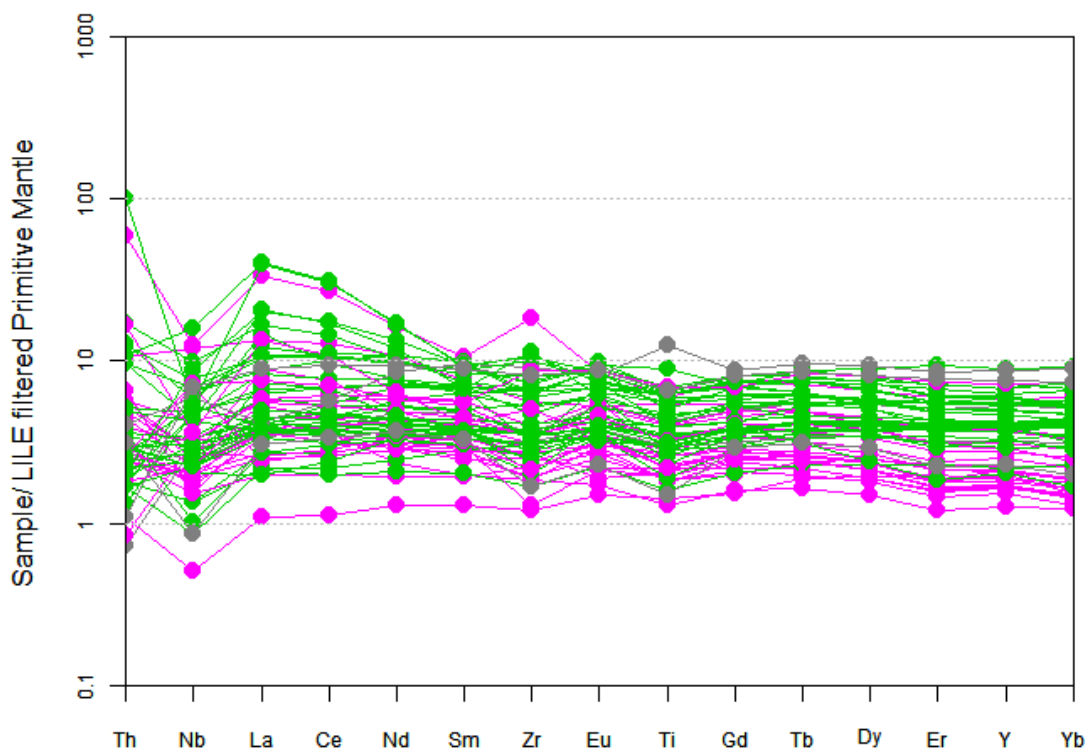


Fig. 15 Primitive mantle normalised trace element spider diagram for the melanocratic to ultramafic rocks. See figure 12 for legend.

Trace element abundances range primarily between 1 to 10 times primitive mantle values, generally with smooth incompatible element patterns (Fig. 15). In detail, however, the REE are varying between depleted and more enriched patterns (Fig. 16). Depleted samples have flat REE with La/Sm_{N} and Gd/Yb_{N} broadly ~ 1 , while some samples have ratios > 1.5 (Fig. 17). The most striking difference between the ultramafic rocks and melanocratic amphibolites are the lower mid to heavy REE abundances in the ultramafic rocks despite similar light REE concentrations (Fig. 16). Nb/La and Nb/Th ranges between crustal ratios and moderately depleted mantle ratios, and Nb/Th is correlated with Nb/La (Fig. 18). Nb/La, Nb/U and Nb/Th for the rocks at Nunatak 1390 plot along systematic arrays between depleted modern mid ocean ridge basalt (MORB) and Archaean tonalite-trondhjemite-granodiorite (TTG) components. The sample with the highest ratios is similar to primitive mantle but has lower ratios than most Archaean greenstone belts (Fig. 19).

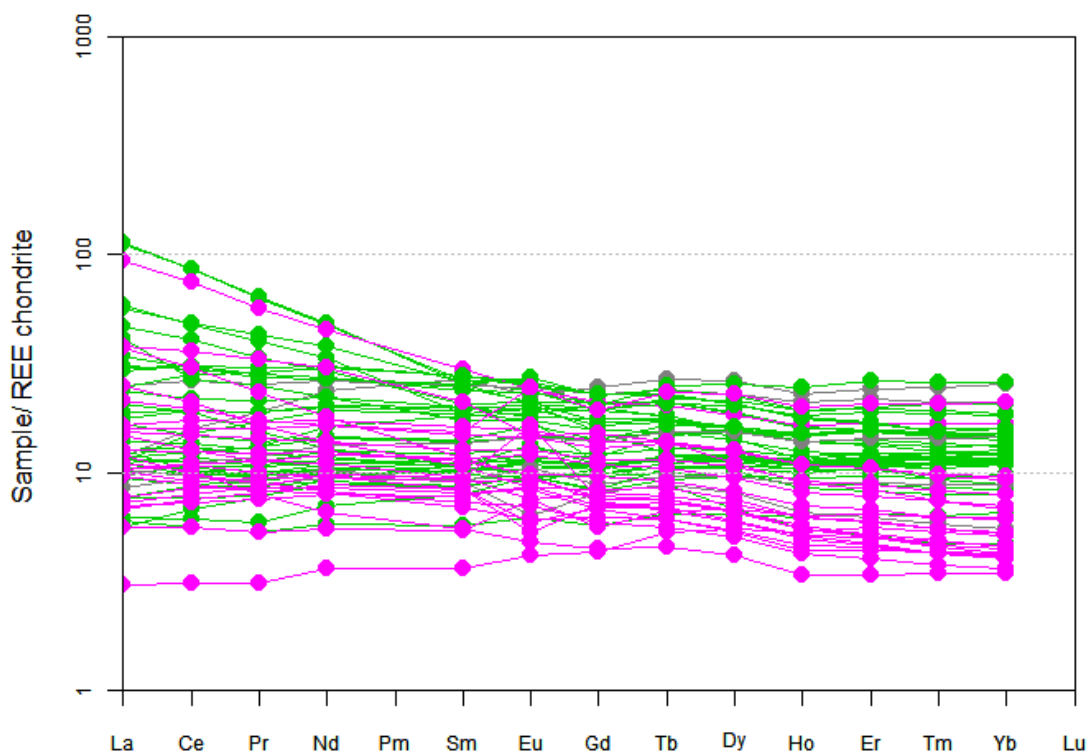


Fig. 16 Chondrite normalised rare earth element (REE) diagram for the melanocratic to ultramafic rocks. See figure 12 for legend.

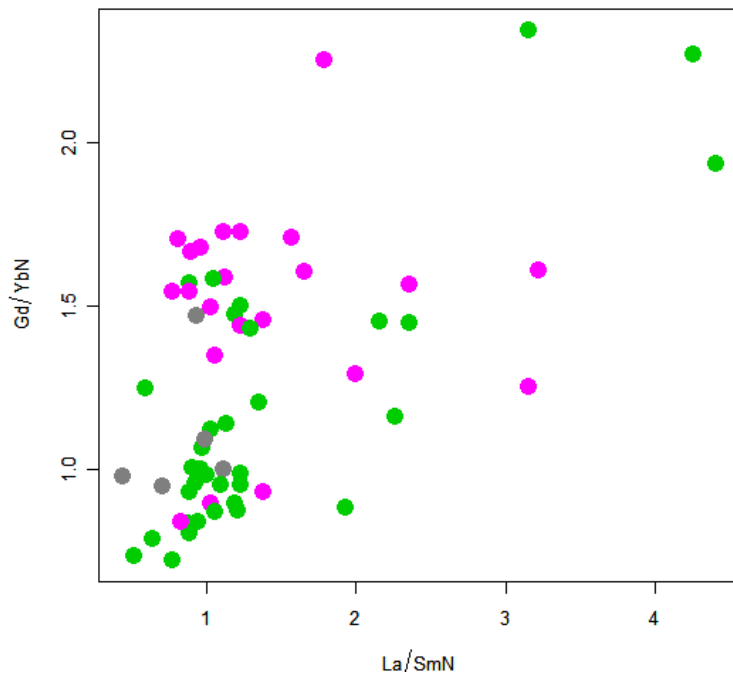


Fig. 17 Chondrite normalised La/Sm plotted against Gd/Yb . La/Sm is similar in both ultramafic and amphibolites, while the ultramafic rocks generally have higher Gd/Yb than the amphibolites. See figure 12 for legend.

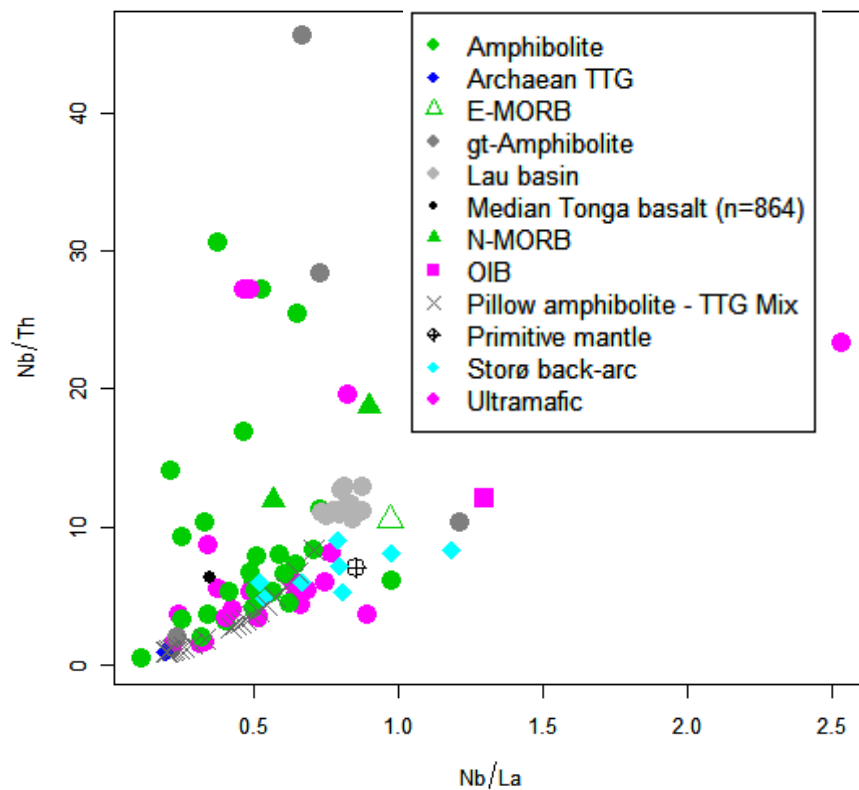


Fig. 18 Nb/La plotted against Nb/Th for the melanocratic to ultramafic rocks. Data sources for Archaean TTG from Martin (1995) and Martin et al. (2005) E-MORB from Klein (2003), Lau basin from Regelous et al. (2008), Tonga basalts from GEOROC (<http://georoc.mpch-mainz.gwdg.de/georoc/>), N-MORB from Hofmann (1988), OIB from Sun and McDonough (1989) and Storø data from van Gool et al. (2008).

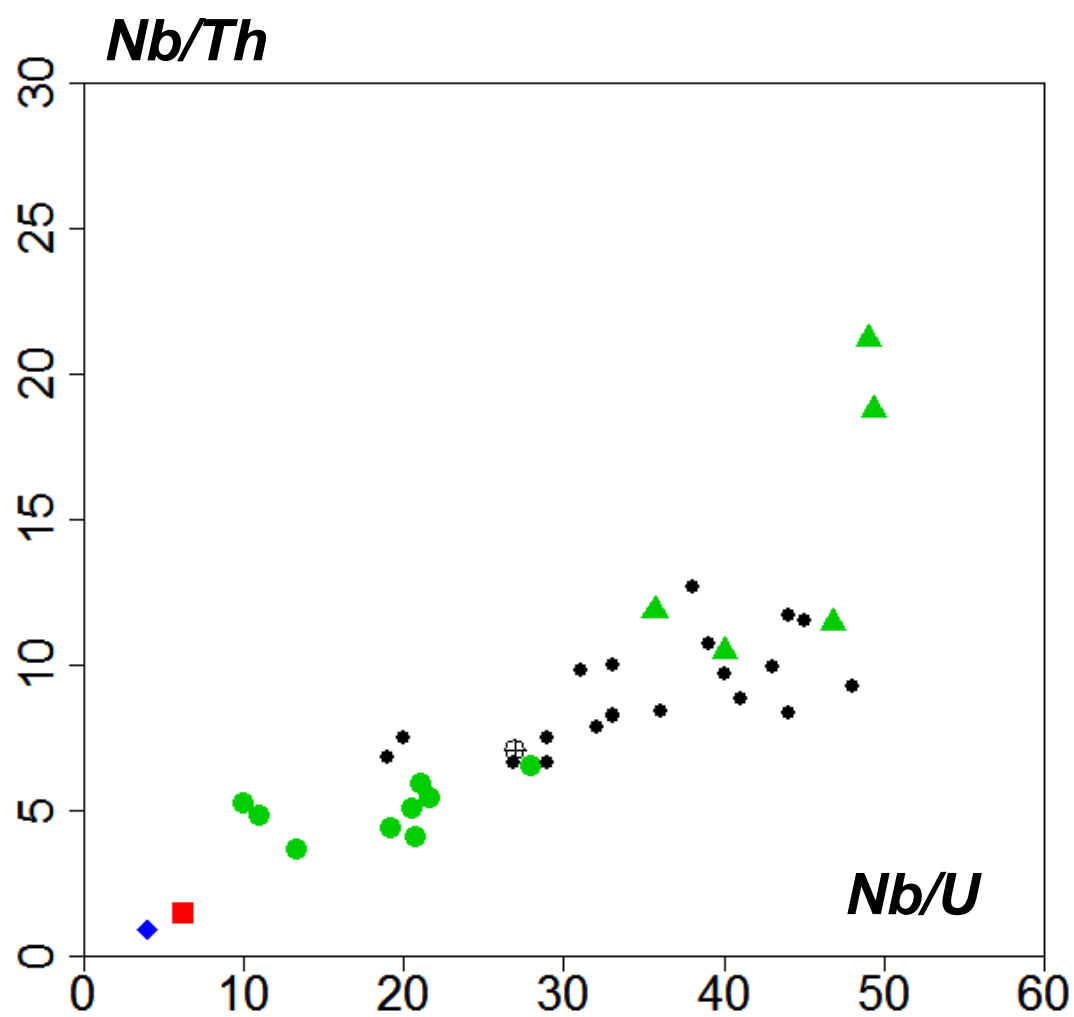


Fig. 19 A plot of Nb/U vs Nb/Th for melanocratic-ultramafic rocks from Nunatak 1390 (green circles), modern MORB (green triangles), primitive mantle (\oplus), bulk continental crust (red square), Archaean greenstone belts (black circles) and mean Archaean tonalite-trondhjemite-granodiorite (TTG) rocks. The mean value for each Archaean greenstone belt is plotted (data from Condie, 2003).

The overall Tasiussarsuaq greenstone data straddle the fields of MORB and island arc tholeiites in tectonic discrimination diagrams such as those deduced by Shervais (1982) or Pearce and Cann (1973) (Fig. 20 & 21). An intra-oceanic arc setting is viable to explain the chemical trends that we observe, but there is evidence for the existence of continental crust by the time these rocks intruded or erupted (c.f. Næraa & Scherstén, 2008; Næraa unpubl. data).

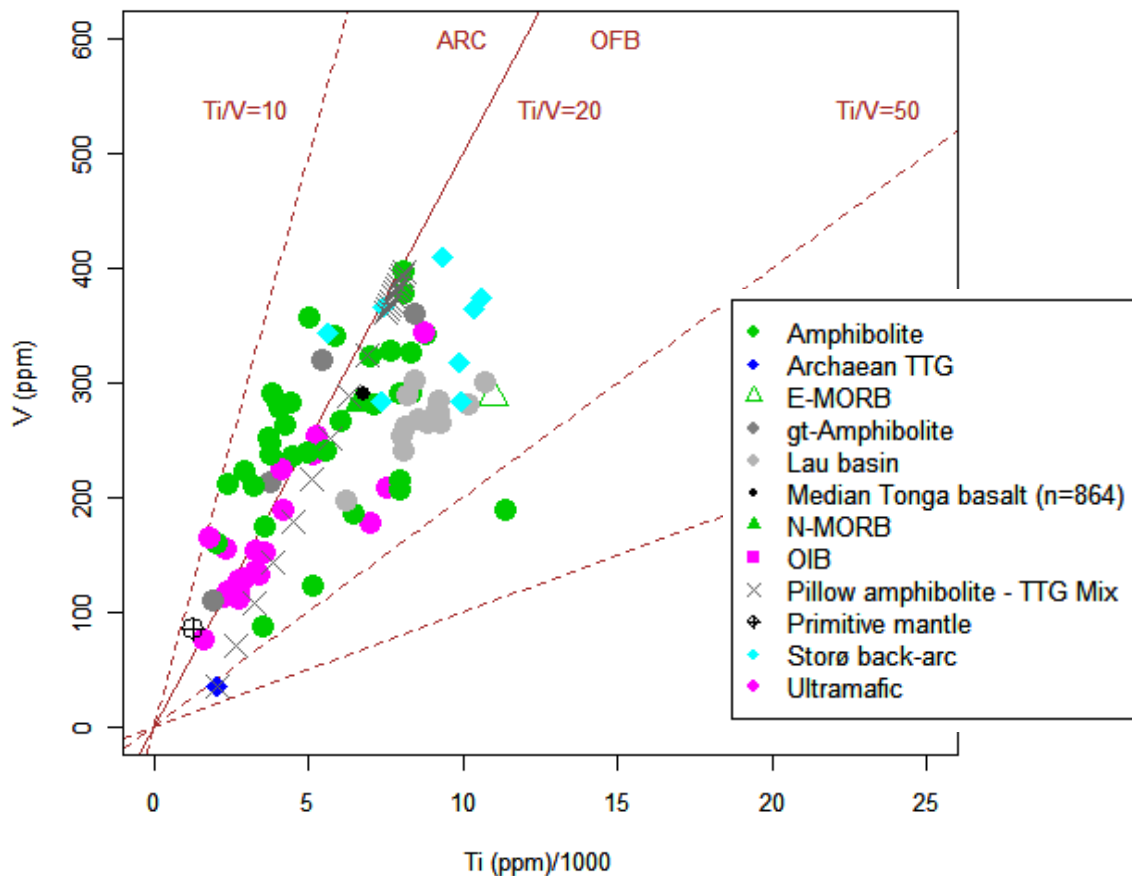


Fig. 20 Ti plotted against V for the melanocratic to ultramafic rocks (Shervais, 1982). Arc denotes typical field for modern arc tholeiites and OFB denotes the typical field for MORB and back-arc basins. Data sources for Archaean TTG from Martin (1995) and Martin et al. (2005) E-MORB from Klein (2003), Lau basin from Regelous et al. (2008), Tonga basalts from GEOROC (<http://georoc.mpch-mainz.gwdg.de/georoc/>), N-MORB from Hofmann (1988), OIB from Sun and McDonough (1989) and Storø data from van Gool et al. (2008).

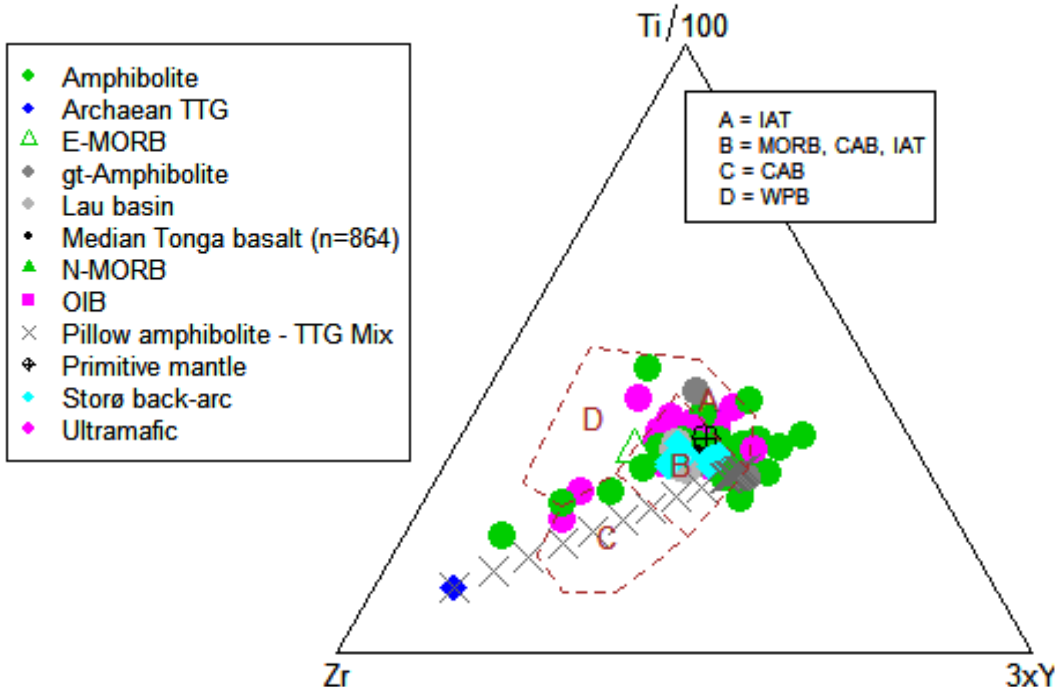


Fig. 21 *Ti-Zr-Y ternary diagram after Pearce & Cann (1973) for the melanocratic to ultramafic rocks. Data sources for Archaean TTG from Martin (1995) and Martin et al. (2005) E-MORB from Klein (2003), Lau basin from Regelous et al. (2008), Tonga basalts from GEOROC (<http://georoc.mpch-mainz.gwdg.de/georoc/>), N-MORB from Hofmann (1988), OIB from Sun and McDonough (1989) and Storø data from van Gool et al. (2008).*

Felsic rocks

Eighteen grey gneisses, granites, and rhyolites were analysed for major and trace element abundances (appendix I). Rock classification is based on field appearance and geochemical composition. The rocks range in SiO_2 from 59.9 to 76.5 wt% on a volatile free basis with a relatively high mean value of 68 ± 6 (± 1 SD) wt%. (Fig. 22) Likewise, these rocks are characterised by relatively high Na_2O that range between 2.7 and 5.0 wt%, with a mean of 4 ± 1 (± 1 SD) wt% (Fig. 22). These features are typical for Archaean tonalite-trondhjemite-granodiorite (TTG) suites (Martin *et al.*, 2005). The majority of the rocks have A/CNK close or slightly higher than unity, i.e. they are weakly peraluminous, except the low SiO_2 rock, which is strongly peraluminous (Fig. 23). Its high A/CNK might result from alteration processes, and the rock is not considered any further.

Felsic rocks are enriched in most incompatible trace element abundances (Fig. 24). Element ratios are similar to Archaean TTG and characterised by lower than mantle Nb/Th , Sm/Zr , and Ti/Gd , high chondrite normalised Gd/Yb_N and typical Y versus Sr/Y (Figs. 24 & 25; Martin *et al.*, 2005). The relatively steep REE patterns noted in the felsic rocks are typical for calc-alkaline rocks, and the patterns are distinctly different from the melanocratic to ultramafic rocks, which are flat (Fig. 16).

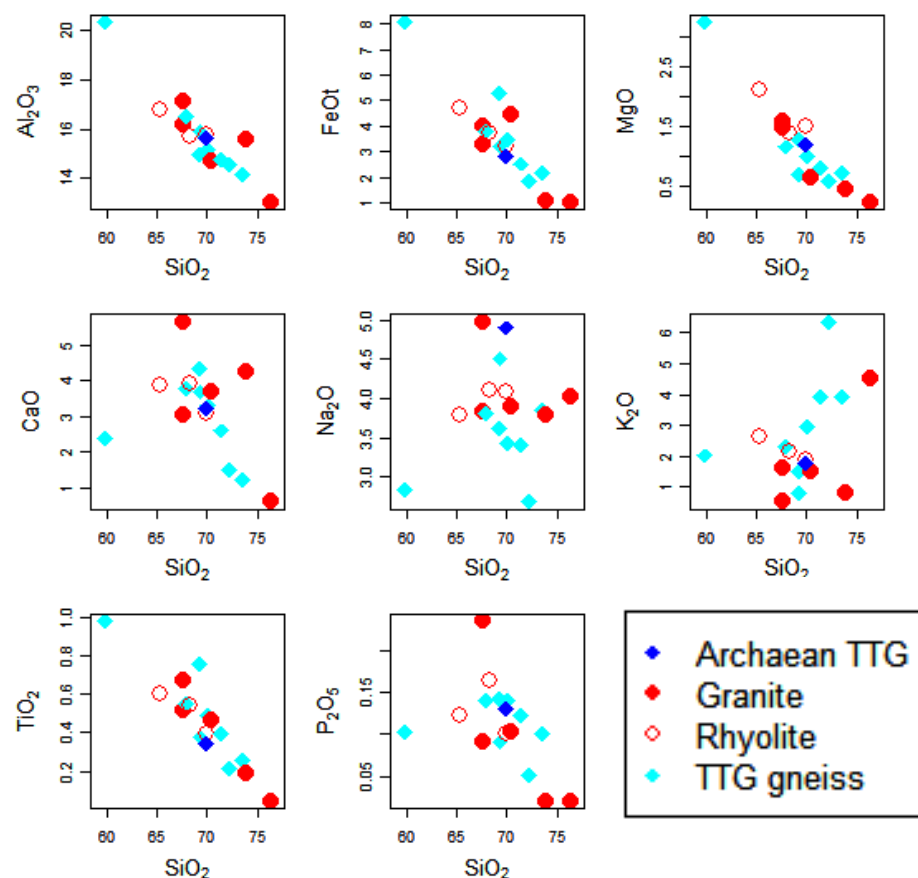


Fig. 22 Major elements plotted against SiO_2 for Tasiussarsuaq felsic grey (TTG) gneisses, granites and rhyolites.

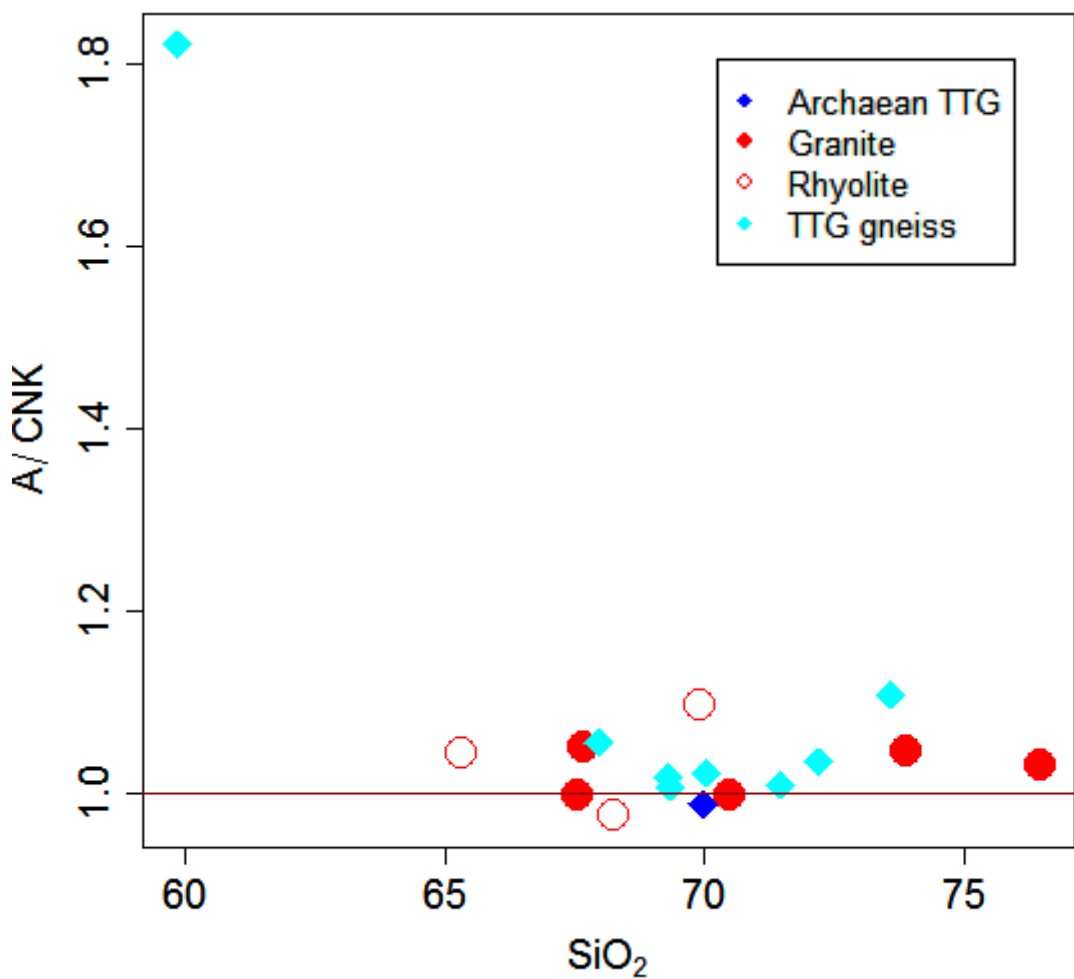


Fig. 23 SiO_2 plotted against A/CNK (i.e. aluminium to calcium and alkali ratio) for Tasiussarsuaq felsic grey (TTG) gneisses, granites and rhyolites. Symbols are same as in figure 20.

The limited data set for the felsic is in keeping with that commonly inferred for Archaean TTG-gneisses, namely slab melts in subduction zones, with variable interaction with the mantle wedge peridotite (Martin *et al.*, 2005).

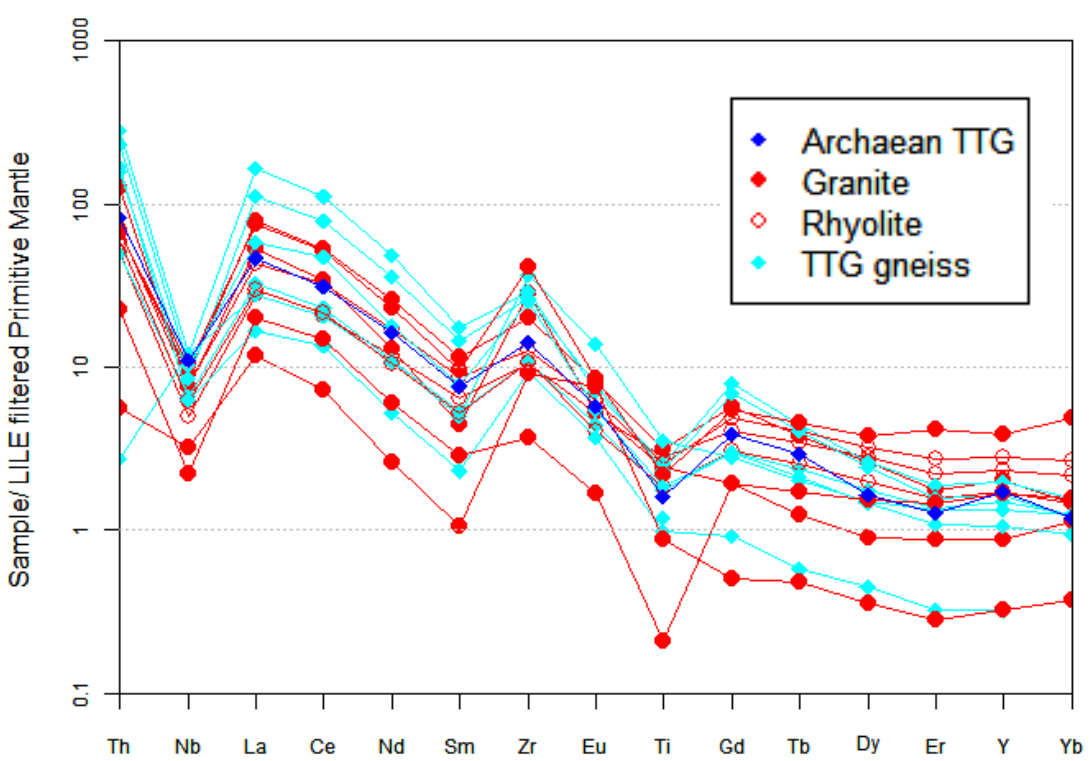


Fig. 24 Primitive mantle normalised trace element variation diagram

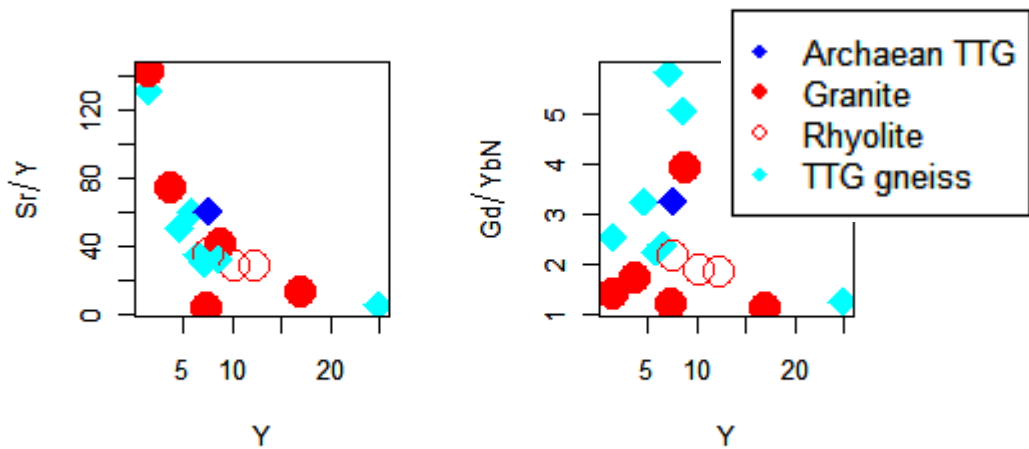


Fig. 25 Sr/Y and Chondrite normalised Gd/Yb plotted against Y .

Discussion

Melanocratic to ultramafic rocks

Major elements

The rocks from Nunatak 1390 appear to be better preserved than most of the Tasiussarsuaq greenstones. Here we make the assumption that the majority of the Tasiussarsuaq greenstones are of the same age and origin as those on Nunatak 1390. The geochemical signature of the different melanocratic to ultramafic complexes within the Tasiussarsuaq terrane are very similar and might suggest the rocks are comagmatic. However, more work is required to test whether this assumption is correct.

The volcanic rocks on Nunatak 1390 consist of a bimodal succession, which was metamorphosed in greenschist facies. The overall preservation of primary volcanic textures and structures is unusual in southern West Greenland. Zircon from a rhyolite yield a $^{207}\text{Pb}/^{206}\text{Pb}$ -age of 2.873 ± 0.005 Ga (Næraa & Scherstén, 2008), which is within the range of the Tasiuarsuaq terrane (2.92–2.86 Ga), and the minimum age for the melanocratic to ultramafic rocks. Two spots in a single zircon grain yield a Concordia age of c. 3.2 Ga and could indicate the presence of older continental crust. It remains unclear, however, if the basalts were emplaced in an oceanic, continental or transient tectonic environment. The indication that there is a ~3.2 Ga basement is suggestive of a continental component and that the melanocratic to ultramafic rocks, which are believed to postdate 3.2 Ga, were emplaced onto this basement, or along adjacent rift basins. The possible existence of an older basement is corroborated by recent unpublished zircon dates around 3.25 Ga further west in the Tasiussarsuaq terrane.

During the mapping in 2007, it was found that there is a cyclic repetition between pillow lava sequences and finely banded melanocratic layers and sheets, which are interpreted as ash layers and flow sheets. Ash layers were previously recognised to overlie the pillow lava, but the cyclic nature between seemingly sub-aqueous and sub-aerial volcanic deposits likely represent conditions that excludes a deep oceanic basin. This is corroborated by the abundant filled vesicles in the pillows, which suggest a low confining pressure during eruption.

Stendal and Scherstén (2007a,b) noted that the ultramafic rocks display pillow lava like structures (Fig. 9), which would imply that they were erupted as liquids with only minor to moderate amounts of cumulus minerals. If correct, the composition of these rocks would require melting pressures ≥ 7 GPa (Walter, 1998). Such high pressure melting is observed in e.g. the 3.4 Ga Barberton komatiites, and a mantle plume origin is commonly invoked to explain the anomalously deep melting. Garnet is stable at such high pressures, and will form a residual phase after melting. Mantle garnet have distinct trace element patterns that should reflect deep melting. For instance, low garnet Gd/Yb values will result in melts with high ratios that are exceeding those of the mantle source, i.e. suprachondritic. Likewise is deeper melting leading to lower $\text{Al}_2\text{O}_3/\text{TiO}_2$ and an anticorrelation between $\text{Al}_2\text{O}_3/\text{TiO}_2$ and

Gd/Yb_N thus expected. The data from camp 1 seems to form two groups, one that tends to be more MgO -rich on average, coupled with $\text{Gd/Yb}_N \sim 1.5$ and $\text{Al}_2\text{O}_3/\text{TiO}_2 < 15$, and the other with lower average MgO -contents, $\text{Gd/Yb}_N \sim 1$ and $\text{Al}_2\text{O}_3/\text{TiO}_2 > 15$. These two groups have completely overlapping trace element ratios and uncorrelated with MgO , or similar fractionation indices.

On Nunatak 1390 at least some of the ultramafic rocks seem to be intercalated with basaltic pillow lavas, which might suggest that they formed sills that are younger than the basalts (Stendal & Scherstén 2007). The higher $\text{Al}_2\text{O}_3/\text{TiO}_2$ ratios of 10–40 for the amphibolites and <10 for the ultramafic eruptives imply a deeper melt origin for the ultramafic rocks that exceeds >5 GPa, i.e. >150 km (Walter 1998). This could imply that the depth of melting increased with time (presuming that the ultramafic rocks are indeed slightly younger than the pillow lavas), or that shallow melting was induced by the deeper melts if they were contemporaneous.

Fractionation of ferro-magnesian minerals will preferentially add or remove FeO and MgO over e.g. CaO , Al_2O_3 and TiO_2 , which are conserved in the residual melt. $(\text{MgO} + \text{FeO}_t)/A$ plotted against SiO_2/A where A is the conserved element should yield a slope of ~0.5 or ~1.2 if olivine or orthopyroxene fractionation is important. Slopes of 0.6 ± 0.3 , 0.98 ± 0.12 and 1.03 ± 0.38 for CaO , Al_2O_3 and TiO_2 , is most consistent with orthopyroxene fractionation, where the lower value for CaO might be caused by slight mobility during metamorphism (Fig. 26). However, the upper ranges of Cr and Ni are within the levels of the mantle, and such high concentrations of these highly compatible elements would require unrealistic amounts of melting. Ni is primarily partitioned into olivine and Cr is strongly enriched in chromite, which can crystallise early in a basic magma. It thus seems that some amount of olivine accumulation is required to explain the compositions of the most MgO rich rocks.

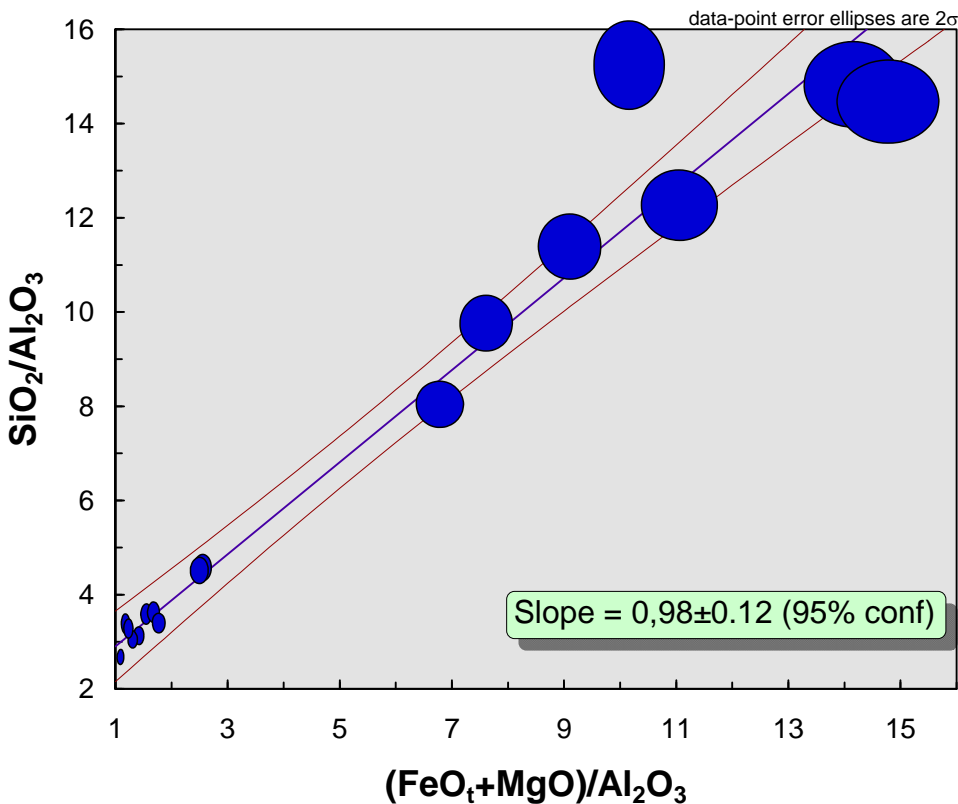


Fig. 26 $(\text{FeO}_t+\text{MgO})/\text{Al}_2\text{O}_3$ plotted against $\text{SiO}_2/\text{Al}_2\text{O}_3$ for samples from Nunatak 1390, with a slope of 0.98 ± 0.12 (95% conf), which is most consistent with orthopyroxene fractionation.

Trace elements

The Tasiusarsuaq ultramafic rocks have smooth trace element patterns, but with Nb/Th ratios that are lower than the primitive mantle (PM; Fig. 27). This implies some degree of enrichment in the mantle source, or that the Nb/Th ratios have decreased due to shallow continental crustal contamination. The light rare-earth element (REE) signatures are horizontal, whereas the mid- to heavy REE signature slopes towards lower abundances, indicating a garnet residue during mantle melting, which is consistent with their deep origin as discussed above (Fig. 27). The REE signatures of the amphibolites are similar to those of the ultramafic rocks, but with slightly higher concentrations, and lacking the garnet signature noted for the ultramafic rocks (Fig. 27). Nb/Th ratios are generally PM-like. Overall, the amphibolites are generally more mid-oceanic ridge basalt (MORB)-like in their range of trace element ratios and abundances. In particular, one core of pillow basalt from Nunatak 1390 consistently lacks continental crustal (or arc-like) trace element patterns.

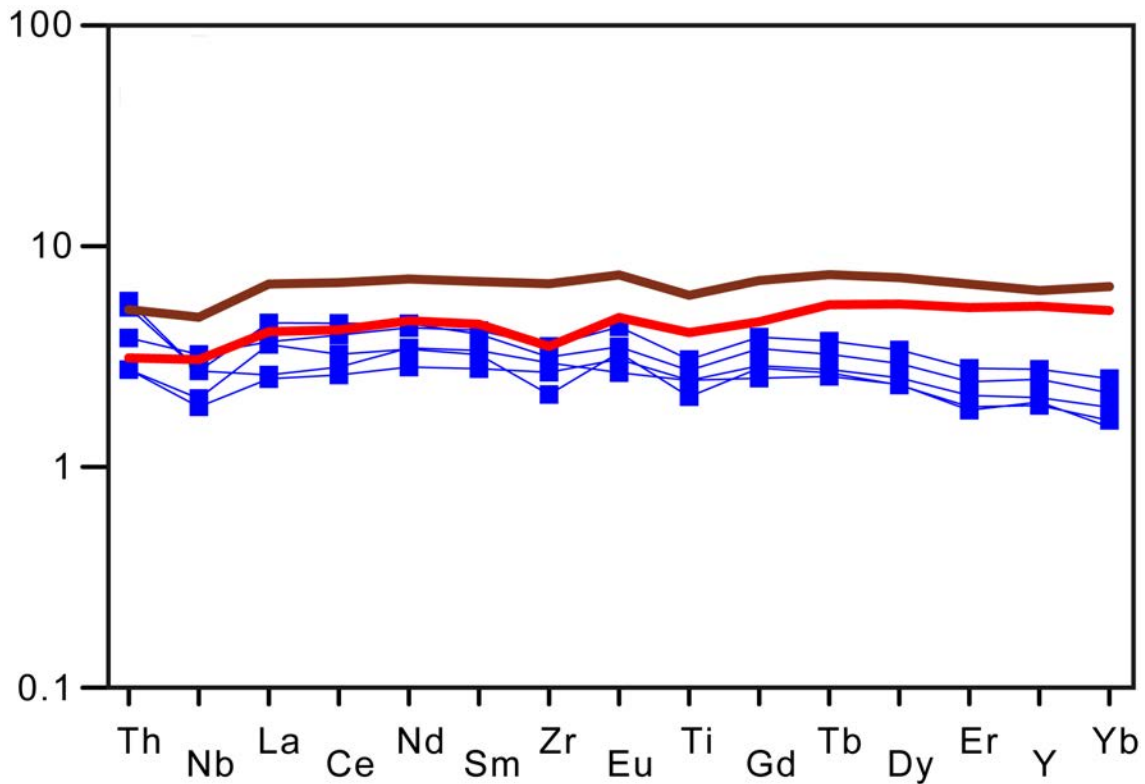


Fig 27 Primitive mantle normalised (Palme & O'Neill, 2003) incompatible trace element diagram for Tasisarsuaq ultramafic rocks (blue squares) in relation to mean Tasisarsuaq amphibolites (red) and pillow lava (brown). See text for discussion.

Nb/U and Nb/Th (Fig. 19) for samples from Nunatak 1390 plot along a mixing curve between depleted mantle ($\text{Nb}/\text{U} = 50$; $\text{Nb}/\text{Th} = 18.7$) and continental crust or TTG-like end-members ($\text{Nb}/\text{U} = 4$; $\text{Nb}/\text{Th} = 0.9$). None of the amphibolites have ratios that are higher than primitive mantle (Fig. 19). At face value, this might be taken to reflect enriched or primitive mantle sources. There is, however, abundant isotopic evidence for extensive depleted mantle sources for a range of Greenland mantle derived rocks (e.g. Bennett et al., 1993; Frei et al., 2004). Furthermore, a global survey of Archaean komatiite suites, suggest that mantle depletion was extensive by 2.7–3.5 Ga (Campbell, 2003). Here we assume the existence of a well mixed global depleted mantle by the time of formation of the greenstones in this survey. It then follows that the enriched Nb/U and Nb/Th must be due to an enriched mantle source, crustal contamination or metamorphic overprinting. The data from the 1390 Nunatak plot along a relatively well defined trend that coincides with the general mixing curve for a depleted mantle – continental crust end-member mixing model (Fig. 19), while data from the region scatter above the mixing line. The scatter in the regional data set is not surprising given the extensive metamorphic overprinting at amphibolite- to granulite facies grade. If it assumed that the scatter is chiefly due to U mobilisation, the co-variation with Th noted at Nunatak 1390 is unexpected as that would imply the same degree of mobility in the same direction, which we consider unlikely. We therefore conclude that U-Th mobility has been insignificant for the Nunatak 1390 samples and that the Nb/U and Nb/Th ratios reflect the source and(or) various degrees of crustal contamination. Based on the global data set of Archaean greenstone belts and the depleted mantle derived rocks in the Archaean basement of Greenland, we assume that

the mantle source of these basalts was depleted with Nb/U and Nb/Th around 35 and 12 respectively. The Nunatak 1390 array is consistent with 1-5% contamination of an average Archaean TTG component. Such a small level of contamination will have an insignificant effect on major elements and isotope ratios and easily pass undetected. It may thus be assumed that the depleted mantle end-member is similar to depleted greenstones of similar age. The task of distinguishing between mantle enrichment processes and local crust contamination is more difficult. For instance, modern oceanic arc basalts are overlapping with the range observed for Archaean greenstones, albeit with a tendency towards lower Nb/U for a given Nb/Th.

The general geochemical signatures and the subaqueous nature of the amphibolites and ultramafic rocks are consistent with an ocean-floor origin in its broadest sense. The MORB-like signatures of the amphibolites might be suggestive of an ocean basin, a back-arc basin or even a primitive tholeiitic arc. However, a major extensional setting such as a mid-ocean ridge is at odds with major simultaneous continental crust formation, which is indicated by e.g. massive volumes of presumably contemporaneous TTG crystallisation (Næraa & Scherstén 2008), while a back-arc basin seems more conceivable. The trace-element arrays indicate source enrichment, i.e. variable amounts of enriched subduction components, or local contamination during emplacement (Fig. 28). Positive correlations for Nb/Th and Nb/La against the Th or La concentration reciprocals lie between mantle and continental crustal end-members, and these ratios are the most sensitive to small degrees of contamination. Assuming a TTG crustal component as the contaminant, the array can be explained by <5% contamination for all but one sample, supposing that the most primitive ultramafic rocks are uncontaminated.

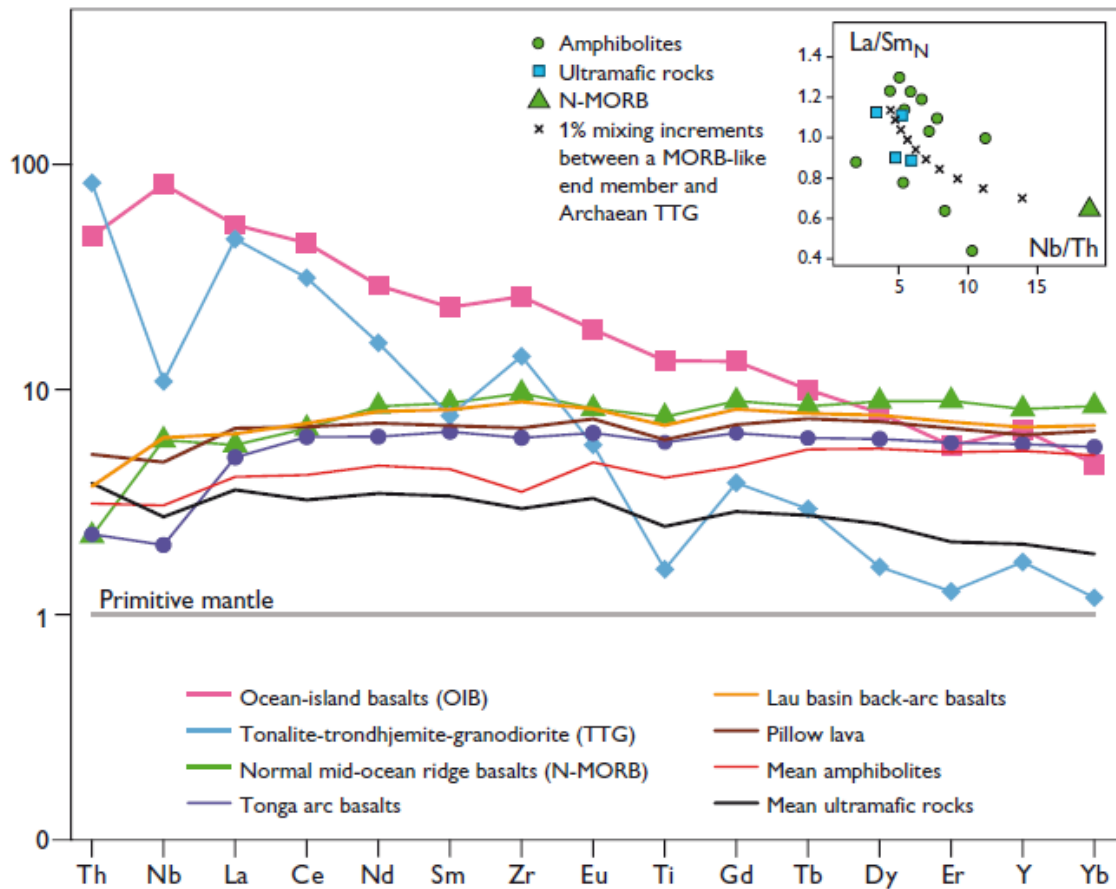


Fig 28 Primitive mantle (Palme & O'Neill 2003) normalised trace element diagram for Tasiussarsuaq greenstones, one pillow lava from Nunatak 1390 and selected reference rocks and reservoirs. For comparison plots of N-MORB (Hofmann 1988), OIB (Sun & McDonough 1989), Archaean TTG (Martin 1995; Martin et al. 2005), Lau basin back-arc (Regelous et al. 2008) and median Tonga arc basalts (<http://georoc.mpch-mainsz.gwdg.de/georoc>) are shown. Inset: N-MORB, Lau basin back-arc basalts and OIB are characterised by Nb/Th ratios that are higher than PM, while median Tonga arc basalts and TTG have ratios that are lower than PM. The Tasiussarsuaq ultramafic rocks and one pillow lava have arc-like ratios lower than PM Nb/Th, while the amphibolites are variable with both sub- and supra-PM ratios. Minor TTG contamination of magmas with MORB-like ratios would rapidly decrease Nb/Th with associated increasing La/Sm, as these ratios are extreme in TTG. A plot of Nb/Th against chondrite normalised La/Sm is shown in the figure inset for the Tasiussarsuaq data, displaying a moderate fit with a mixing scenario as discussed above.

Summary

If the basalt–komatiite magmatism in the Tasiussarsuaq terrane is indeed concurrent with TTG-formation, an arc or back-arc environment for the former magmatism is favoured (cf. Stendal & Scherstén 2007; Næraa & Scherstén 2008), and such a hypothesis is still viable in the light of the current geochemical data. The origin of komatiites remains controversial, although most authors advocate a mantle-plume related origin. The komatiite-like rocks documented here do not readily fit such an origin as they seem to be primarily associated

with subduction and growth of continent crust. Alternatively, renewed models for subduction-related komatiite genesis might be considered. However, this scenario typically involves shallow melting (Grove & Parman 2004), while the REE ratios observed here favour deep melting with residual garnet.

Acknowledgements

Financial support from the Greenland Bureau of Mineral and Petroleum is acknowledged. We thank Tomas Næraa, Adam Garde and Lotte Melchior Larsen for discussions over the past years. Denis Schlatter provided a detailed review that improved the report.

References

- Allaart, J.H. 1982: Geologisk kort over Grønland, 1:500 000, Sheet 2 Frederikshåb Isblink - Søndre Strømfjord. Copenhagen: Grønlands Geologiske Undersøgelse.
- Appel, P.W.U., Garde, A.A., Jørgensen, M.S., Moberg, E.D., Rasmussen, T.M., Schjødt, F. & Steenfelt, A. 2003: Preliminary evaluation of the economic potential of the greensone belts in the Nuuk region. Danmarks og Grønlands Geologiske Undersøgelse Rapport 2003/94, 147pp.
- Appel, P.W.U., Coller, D., Coller, V., Heijlen, W., Moberg, E.D., Polat, A., Raith, J., Schjødt, F., Stendal, H. & Thomassen, B. 2005: Is there a gold province in the Nuuk region? Report from field work carried out in 2004. Danmarks og Grønlands Geologiske Undersøgelse Rapport **2005/27**, 79pp.
- Bennett, V.C., Nutman A.P. & McCulloch, M.T. 1993: Nd-isotopic evidence for transient, highly depleted mantle reservoirs in the early history of the Earth. *Earth and Planetary Science Letters* **119**, 299-317.
- Campbell, I.H. 2003: Constraints on continental growth models from Nb/U ratios in the 3.5 Ga Barberton and other Archaean basalt-komatiite suites.. *American Journal of Science*, **303**, 319-351.
- Chadwick, B. & Coe, K. 1983: Buksefjorden 63 V.1 Nord. Descriptive text. Geological map of Greenland 1:100 000. The regional geology of a segment of the Archaean block of southern West Greenland., 70. Copenhagen: Grønlands Geologiske Undersøgelse.
- Condie, K.C. 2003: Incompatible element ratios in oceanic basalts and komatiites: Tracking deep mantle sources and continental growth rates with time. *Geochemistry, Geophysics, Geosystems*, **4**, doi:10.1029/2002GC000333.
- Crowley, J.L. 2002: Testing the model of late Archean terrane accretion in southern West Greenland: a comparison of the timing of geological events across the Qarliit nunaat fault, Buksefjorden region. *Precambrian Research* **116**, 57-79.
- Eilu, P., Garofalo, P., Appel, P.W.U. & Heijlen, W. 2006: Alteration patterns in Au-mineralised zones of Storø, Nuuk region - West Greenland, 73 pp Geological Survey of Denmark and Greenland, Copenhagen, 2006/30).
- Escher, J.C. 1981: Geologisk kort over Grønland 1:100 000 63 V.2 Nord Kangiata nuna 63°30'–64°00'N; 49°00'–50°42'W. Copenhagen: Grønlands Geologiske Undersøgelse.
- Escher, J.C. & Myers, J.S. 1975: New evidence concerning the original relationships of early Precambrian volcanics and anorthosites in the Fiskenæsset region, southern West Greenland. Rapport Grønlands Geologiske Undersøgelse, **75**, 72–76.
- Escher, J.C. & Pidgeon, R.T. 1976: Field mapping of nunatak 1390 m, east of Alángordlia, southern West Greenland. Rapport Grønlands Geologiske Undersøgelse, **80**, 84–87. Copenhagen: Grønlands Geologiske Undersøgelse.
- Escher, J.C. & Pulvertaft, T.C.R. 1995: Geological map of Greenland, 1:2 500 000. Copenhagen: Geological Survey of Greenland.
- Fitton, J.G., Saunders, A.D., Norry, M.J., Hardarson, B.S. & Taylor, R.N. 1997: Thermal and chemical structure of the Iceland plume. *Earth and Planetary Science Letters* **153**, 197-208.

- Frei, R., Polat, A. & Meibom, A. 2004: The Hadean upper mantle conundrum: Evidence for source depletion and enrichment from Sm-Nd, Re-Os, and Ph isotopic compositions in 3.71 Gy boninite-like metabasalts from the Isua Supracrustal Belt, Greenland. *Geochimica et Cosmochimica Acta* **68**, 1645-1660.
- Friend, C.R.L. & Nutman, A.P. 2001: U - Pb zircon study of tectonically bounded blocks of 2940 - 2840 Ma crust with different metamorphic histories, Paamiut region, South-West Greenland: implications for the tectonic assembly of the North Atlantic craton. *Precambrian Research* **105**, 143 - 164.
- Friend, C.R.L. & Nutman, A.P. 2005: New pieces to the Archaean terrane jigsaw puzzle in the Nuuk region, southern West Greenland: steps in transforming a simple insight into a complex regional tectonothermal model. *Journal of the Geological Society, London* **162**, 147 - 162.
- Garde, A.A. 1989: Geologisk kort over Grønland, 1:100 000, Fiskefjord, 64 V. 1 Nord. Copenhagen: Grønlands Geologiske Undersøgelse.
- Garde, A.A. 1997: Arkæisk skorpedannelse i et højmetamorf grundfjeldsområde, Fiskefjordregionen, Vestgrønland. (In Danish.) Danmarks og Grønlands Geologiske Undersøgelse Rapport **1997/125**, 19 pp.
- Garde, A.A. 2007: A mid-Archaean island arc complex in the eastern Akia terrane, Godthåbsfjord, southern West Greenland. *Journal of the Geological Society, London*, **164**, 565–579.
- Grove, T.L. & Parman, S.W. 2004: Thermal evolution of the Earth as recorded by komatiites. *Earth and Planetary Science Letters* **219**, 173–187.
- Hofmann, A.W. 1988: Chemical differentiation of the Earth - the relationship between mantle, continental-crust, and oceanic-crust. *Earth and Planetary Science Letters* **90**, 297-314.
- Hollis, J.A., van Gool, J.A.M., Steenfelt, A. & Garde, A.A. 2004: Greenstone belts in the central Godthåbsfjord region, southern West Greenland. Danmarks og Grønlands Geologiske Undersøgelse Rapport **2004/110**, 110 pp.
- Hollis, J.A.(ed.) 2005: Greenstone belts in the central Godthåbsfjord region, southern West Greenland. Danmarks og Grønlands Geologiske Undersøgelse Rapport **2005/42**, 215pp.
- Hollis, J.A., Schmid, S., Stendal, H., van Gool, J.A.M. & Weng, W.L. 2006: Supracrustal belts in Godthåbsfjord region, southern West Greenland. Progree report on 2005 field work: geological mapping, regional hydrothermal alteration and tectonic sections, 171 pp plus 1 DVD, Geological Survey of Denmark and Greenland, Copenhagen, 2006/7).
- Jensen, L.S. 1976: A new cation plot for classifying subalkalic volcanic rocks. Ontario Division of Mines, Miscellaneous Paper **66**, 22pp.
- Kemp A.I.S. and Hawkesworth, C.J. 2003: Granitic perspectives on the generation and secular evolution of the continental crust. In *Treatise on Geochemistry* **12**, The Crust (ed. R. Rudnick) Elsevier Science, Oxford, 349-410.
- Klein, E.M. 2003: Geochemistry of the Igneous Oceanic Crust. In *Treatise on Geochemistry* **13**, The Crust (ed. R. Rudnick) Elsevier Science, Oxford, 433-463.
- Kolb, J. & Stendal, H. 2007: Geological environments and hydrothermal mineralisation in Nunataarsuk, Qarliit Nunaat and Ameralik, Nuuk region, SW Greenland - a field report 2007. Mineral resource assessment of the Archaean Craton SW Greenland Contribution no 2. Danmarks og Grønlands Geologiske Undersøgelse Rapport **2007/58**, 44 pp.

- Martin, H. 1995: Archean grey gneisses and the genesis of continental crust. In: Condie, K.C. (ed.): Archean crustal evolution, 205–260. Amsterdam: Elsevier.
- Martin, H., Smithies, R.H., Rapp, R., Moyen, J.F. & Champion, D. 2005: An overview of adakite, tonalite-trondhjemite-granodiorite (TTG), and sanukitoid: relationships and some implications for crustal evolution. *Lithos* **79**, 1-24.
- McGregor, V.R. 1984: Geologisk kort over Grønland 1:100 000 64 V.1 Syd Qôrqu 64°00' – 64°30'N; 50°45' – 52°30'W;
- McGregor, V.R. 1993: Geological map of Greenland 1:100 000. Descriptive text. Qôrqu 64 V.1 Syd. The regional geology of part of the Archaean block of southern West Greenland, including a segment of the late Archaean mobile belt through Godthåbsfjord., 40. Copenhagen: Grønlands Geologiske Undersøgelse.
- Naeraa, T. & Scherstén, A. 2008: New zircon ages from the Tasiussarsuaq terrane, southern West Greenland. *Geological Survey of Denmark and Greenland Bulletin* **15**, 73–76.
- Nielsen, B.M., Rasmussen, T.M. & Steenfelt, A. 2004: Gold potential of the Nuuk region based on multiparameter spatial modelling of known gold showings. Interim report 2004. Danmarks og Grønlands Geologiske Undersøgelse Rapport **2004/121**, 155pp.
- Palme, H. & O'Neill, H. St.C., 2003: Cosmochemical Estimates of Mantle Composition. In Treatise on Geochemistry **2**, (ISBN: 0-08-044337-0), 1–38
- Pearce, J.A., Cann, J.R., 1973. Tectonic setting of basic volcanic-rocks determined using trace-element analyses. *Earth and Planetary Science Letters* **19** (2), 290–300.
- Regelous, M., Turner, S., Falloon, T.J., Taylor, P., Gamble, J. & Green, T. 2008: Mantle dynamics and mantle melting beneath Niuafo'ou Island and the northern Lau back-arc basin. *Contributions to Mineralogy and Petrology*. DOI: 10.1007/s00410-007-0276-7.
- Schiøtte, L., Compston, W. & Bridgwater, D. 1989: U-Pb single-zircon age for the Tinissaq gneiss of southern West Greenland - a controversy resolved. *Chemical Geology* **79**, Pages: 21-30.
- Shervais, J.W. 1981: Ti-V plots and the petrogenesis of modern and ophiolitic lavas. *Earth and Planetary Science Letters* **59**, 101-118.
- Stendal, H. (ed.) 2007: Characterisation of selected geological environments. Mineral resource assessment of the Archaean Craton (66° to 63°30'N) SW Greenland contribution no. 1. Danmarks og Grønlands Geologiske Undersøgelse Rapport 2007/20, 90 pp.
- Stendal, H. & Scherstén, A. 2007a: A well-preserved bimodal Archaean volcanic succession in the Tasiussarsuaq terrane, South-West Greenland. *Geological Survey of Denmark and Greenland Bulletin* **13**, 53-56.
- Stendal, H. & Scherstén, A. 2007b: Geological Environments: Oceanic crust and hydrothermal alterations - Field report 2006. In: Stendal, H. (ed.): Characterisation of selected geological environments. Mineral resource assessment of the Archaean Craton SW Greenland. Contribution no. 1 **2007/20**, 59-88 Danmarks og Grønlands Geologiske Undersøgelse Rapport.
- Stensgaard, B.M., Steenfelt, A. & Rasmussen, T.M. 2006: Gold potential of the Nuuk region based on multiparameter spatial modelling, 207 pp Geological Survey of Denmark and Greenland, Copenhagen, 2006/27).
- Sun, S.-s. & McDonough, W.F. 1989: Chemical and isotopic systematics of oceanic basalts: implications for mantle compositions and processes. In: Saunders, A.D. & Norry, M.J. (eds.): Magmatism in the Ocean Basins. Geological Society Special Publications no. 42, pp. 313-345.

van Gool, J.A.M., Scherstén, A., Østergaard, C. & Næraa, T. (2008). Geological setting of the Storø gold prospect, Godthåbsfjord region, southern West Greenland: Results of detailed mapping, structural analysis, geochronology and geochemistry. Danmarks & Grønlands Geologiske Undersøgelse Rapport **2008/83**, 158 pp.

Walter, M.J. 1998: Melting of garnet peridotite and the origin of komatiite and depleted lithosphere. *Journal of Petrology* **39**, 29-60.

Sample	Locality	Camp	Rock class	Symbol	Colour
499104	2006HST286	1	Amphibolite	16	3
499105	2006HST287	1	Amphibolite	16	3
499106	2006HST288	1	Ultramafic	16	6
499108	2006HST293	1	Amphibolite	16	3
499109	2006HST297	1	Ultramafic	16	6
499110	2006HST297	1	Ultramafic	16	6
499112	2006HST297	1	Ultramafic	16	6
499113	2006HST298	1	Ultramafic	16	6
499114	2006HST300	1	Amphibolite	16	3
499115	2006HST300	1	Amphibolite	16	3
499117	2006HST303	1	Amphibolite	16	3
499121	2006HST308	1	Ultramafic	16	6
499122	2006HST309	1	Ultramafic	16	6
499125	2006HST313	1	Amphibolite	16	3
499127	2006HST322	1	Amphibolite	16	3
499128	2006HST324	1	Amphibolite	16	3
499130	2006HST326	1	Amphibolite	16	3
499131	2006HST331	1	Amphibolite	16	3
499132	2006HST332	1	Amphibolite	16	3
499133	2006HST333	1	Ultramafic	16	6
499134	2006HST337	1	Amphibolite	16	3
499136	2006HST339	1	Ultramafic	16	6
499137	2006HST342	1	Ultramafic	16	6
499138	2006HST347	1	Amphibolite	16	3
499139	2006HST348	1	Amphibolite	16	3
499141	2006HST351	1	Amphibolite	16	3
499143	2006HST354	1	Ultramafic	16	6
499146	2006HST362	2	gt-Amphibolite	16	15
499150	2006HST370	2	Amphibolite	16	3
499160	2006HST384	2	Ultramafic	16	6
499169	2006HST400	2	Ultramafic	16	6
499170	2006HST401	2	Amphibolite	16	3
499171	2006HST408	2	Ultramafic	16	6
499172	2006HST410	2	Ultramafic	16	6
499174	2006HST418	2	Amphibolite	16	3
499175	2006HST418	2	Ultramafic	16	6
499176	2006HST425	3	Amphibolite	16	3
499181	2006HST430	3	Amphibolite	16	3
499182	2006HST431	3	Amphibolite	16	3
499183	2006HST432	3	Amphibolite	16	3
499184	2006HST433	3	Amphibolite	16	3
499188	2006HST437	3	Ultramafic	16	6
499189	2006HST437	3	Amphibolite	16	3
499191	2006HST438	3	Ultramafic	16	6
499192	2006HST439	3	Amphibolite	16	3
499196	2006HST441	Reco	gt-Amphibolite	16	15
499201	2006HST443	Reco	gt-Amphibolite	16	15
499202	2006HST444	Reco	gt-Amphibolite	16	6
499207	2006HST452	Reco	Ultramafic	16	6
499209	2006HST456	Reco	Amphibolite	16	3
499214	2006HST462	Reco	Ultramafic	16	6
499216	2006HST463	Reco	gt-Amphibolite	16	15
499218	2006HST467	Reco	Amphibolite	16	3
499219	2006HST468	Reco	Amphibolite	16	3
499222	2006HST469	Reco	Ultramafic	16	6
499223	2006HST469	Reco	Amphibolite	16	3

499224	2006HST470	Reco	Amphibolite	16	3
499226	2006HST471	Reco	Amphibolite	16	3
499231	2006HST474	Reco	Amphibolite	16	3
499232	2006HST474	Reco	Amphibolite	16	3
499247	2006HST499	Reco	gt-Amphibolite	16	15

SiO₂	Al₂O₃	Fe₂O₃	FeOt	MnO	MgO	CaO	Na₂O	K₂O
49,53	13,76	14,78	13,30	0,21	8,52	10,05	1,75	0,29
48,52	13,64	13,82	12,44	0,23	7,55	11,26	2,04	0,39
43,78	5,46	16	14,40	0,22	21,11	8,83	0,85	0,12
48,25	15,92	11,36	10,22	0,18	10,17	10,6	1,82	0,21
46,44	3,05	12,81	11,53	0,23	18,19	16,39	0,42	0,12
48,34	2,95	13,17	11,85	0,2	27,19	5,6	0,24	1,05
46,28	4,75	14,64	13,17	0,23	21,53	10,18	0,23	0,07
47,58	7,67	14,99	13,49	0,24	12,25	13,1	1,48	0,19
63,49	16,42	5,67	5,10	0,08	2,32	7,3	3,31	0,37
46,56	15,06	14,78	13,30	0,21	6,96	11,4	2,18	0,1
48,24	15,99	13,3	11,97	0,17	7,88	10,17	2,45	0,46
49,82	6,49	13,77	12,39	0,24	13,03	13,75	1,61	0,22
42,66	2,95	14,83	13,34	0,24	28,71	8,81	0,19	0,04
47,4	10,56	18,37	16,53	0,32	8,16	11,56	1,69	0,46
50,24	15,46	10,8	9,72	0,17	8,52	11,36	2,14	0,22
51,42	17,58	9,48	8,53	0,16	4,12	9,37	4,07	0,45
45,43	17,16	12,14	10,92	0,19	6,91	14,16	1,39	< 0,01
37,54	15,47	16,95	15,25	0,21	7,43	16,17	0,64	0,31
49,29	10,59	16,78	15,10	0,27	6,56	12,69	2,39	0,16
48,66	6,31	14,69	13,22	0,22	12,56	14,58	1,18	0,26
47,66	14,13	10,75	9,67	0,18	14,59	9,34	1,18	0,34
46,49	4,09	15,72	14,14	0,24	21,54	10,1	0,56	0,15
45,46	3,71	13,56	12,20	0,23	27,47	8,21	0,23	0,12
48,57	14,48	9,99	8,99	0,2	7,47	16,67	1,26	0,19
48,59	14,15	14,57	13,11	0,19	8,96	10,48	1,71	0,03
46,82	10,31	18,68	16,81	0,35	7,83	12,18	1,62	0,38
44,16	2,98	13,8	12,42	0,22	28,35	8,21	0,32	0,05
56,14	15,38	14,49	13,04	0,22	2,45	9,13	0,71	0,16
49,36	14,77	12,2	10,98	0,19	8,08	11,14	2,44	0,47
42,42	19,55	13,39	12,05	0,19	7,34	8,24	2,18	0,09
47,39	4,08	14,35	12,91	0,22	20,52	8,83	0,17	0,1
50,57	13,05	15,32	13,79	0,23	6,52	9,83	2,1	0,61
48,2	5,41	13,73	12,35	0,24	16,22	9,45	0,43	0,6
50,36	3,18	13,08	11,77	0,19	19,19	10,02	0,27	< 0,01
51,66	12,16	11,41	10,27	0,23	9,76	12,33	0,7	0,04
50,1	7,22	9,67	8,70	0,16	19,79	6,92	0,4	2,17
49,8	11,09	13,97	12,57	0,22	8,44	11,64	1,54	0,78
51,29	14,04	11,28	10,15	0,2	7,87	10,65	1,63	0,13
47,46	16,37	13,41	12,07	0,19	7,11	9,52	1,83	0,31
53,39	14,97	11,95	10,75	0,17	5,27	9,55	2,77	0,18
52,42	13,82	11,46	10,31	0,19	7,86	10,37	2,06	0,23
47,96	2,94	13,3	11,97	0,2	21,09	7,02	0,34	0,1
52,73	14,22	15,71	14,14	0,19	4,51	5,44	4,34	0,16
38,44	3,97	14,87	13,38	0,24	22,9	5,97	0,05	< 0,01
55,12	17,66	7,27	6,54	0,09	3,19	5,19	4,13	3,03
78,06	7,04	5,08	4,57	0,08	2,86	2,8	0,28	1,51
50,36	11,68	20,63	18,56	0,26	4,96	7,83	1,27	0,32
53,1	20,93	10,95	9,85	0,17	3,82	4,8	3,18	0,92
50,75	6,81	11,2	10,08	0,17	22,02	5,54	1,5	0,54
48,82	15,75	11,05	9,94	0,18	8,81	10,74	2,71	0,44
47,33	8,4	11,33	10,19	0,16	22,92	7,54	0,77	0,15
47,32	14,71	13,41	12,07	0,24	7,48	14,38	1,29	0,39
50,78	14,58	12,86	11,57	0,16	5,87	8,04	3,14	1,44
49,31	14,78	11,77	10,59	0,18	8,53	11,93	2,39	0,23
41,95	2,12	15,8	14,22	0,24	34,65	4,14	0,39	0,02
50,35	14,6	10,57	9,51	0,2	9,22	11,56	2,37	0,5

46,07	18,48	10,97	9,87	0,16	9,64	11,15	1,98	0,37
48,62	13,45	16,07	14,46	0,24	7,3	10,75	2,11	0,25
47,94	13,84	12,24	11,01	0,21	7,75	13,26	2,27	0,77
48,45	13,91	12,57	11,31	0,2	8,11	11,69	2,57	0,9
47,76	16,28	11,76	10,58	0,19	8,88	11,95	1,15	0,38

TiO ₂	P ₂ O ₅	LOI	Total	V	Cr	Co	Ni
0,831	0,06	0,097	99,88	357	70	55	70
0,948	0,07	1,158	99,62	341	300	55	130
1,119	0,08	1,856	99,43	177	1540	103	1080
0,535	0,05	0,192	99,28	210	270	57	110
0,472	0,03	0,99	99,14	129	1480	106	1240
0,403	0,02	0,876	100	114	1700	116	1490
0,584	0,04	0,927	99,46	152	1730	109	1160
0,831	0,05	0,337	98,73	237	940	79	300
0,583	0,21	0,312	100,1	87	110	17	50
1,316	0,11	0,408	99,07	397	160	57	130
0,992	0,08	0,263	100	266	160	59	180
0,675	0,05	0,088	99,74	225	1350	69	290
0,376	0,02	1,19	100	113	2160	129	1710
1,441	0,11	0,212	100,3	342	380	78	190
0,663	0,05	0,536	100,2	282	220	48	130
1,051	0,22	1,462	99,37	186	50	27	20
0,619	0,04	2,304	100,3	291	330	49	60
1,311	0,13	2,7	98,86	326	110	70	70
1,175	0,09	0,131	100,1	280	80	68	110
0,858	0,05	0,102	99,47	253	840	79	320
0,335	0,03	1,518	100	160	430	70	190
0,542	0,04	0,778	100,2	153	1860	114	1280
0,389	0,02	0,852	100,3	118	1940	123	1760
0,394	0,03	0,498	99,75	211	330	44	70
1,155	0,08	0,264	100,2	323	80	50	100
1,355	0,1	0,223	99,86	291	270	74	180
0,436	0,03	0,64	99,2	115	1700	124	1710
1,394	0,12	0,29	100,5	359	50	66	60
0,818	0,07	0,17	99,7	238	330	49	140
1,18	0,21	4,56	99,35	208	210	49	110
0,526	0,03	3,39	99,63	135	1790	102	1120
1,253	0,13	0,66	100,3	327	190	56	100
0,654	0,05	4,44	99,42	188	1730	81	540
0,444	0,01	2,63	99,37	128	1550	86	940
0,611	0,05	1,04	99,98	251	580	54	80
0,293	0,03	3,26	100	165	2780	80	920
0,905	0,08	1,42	99,89	241	490	56	130
0,607	0,06	1,69	99,45	237	480	52	120
1,279	0,1	1,69	99,27	291	230	50	120
1,309	0,12	0,49	100,2	207	100	35	50
0,622	0,06	0,83	99,91	247	470	53	120
0,527	0,04	5,65	99,15	133	1700	93	1110
1,297	0,13	0,49	99,22	215	100	51	90
0,395	0,03	12,05	98,91	111	3070	128	1000
0,827	0,19	3,59	100,3	123	30	21	20
0,313	0,04	0,8	98,85	110	850	39	250
2,606	0,12	0,19	100,2	868	< 20	43	40
1,439	0,05	0,68	100	343	480	56	190
0,456	0,06	1,1	100,2	118	3170	73	820
0,672	0,02	1,05	100,2	278	370	52	150
0,384	0,02	1,38	100,4	155	2570	83	850
0,902	0,07	0,09	100,3	320	360	57	160
1,853	0,13	0,83	99,67	188	120	42	110
0,741	0,06	0,53	100,4	236	350	51	160
0,267	0,02	0,86	100,5	76	2280	149	2020
0,486	0,04	0,26	100,1	222	270	43	80

0,595	0,05	0,73	100,2	175	90	56	250
1,331	0,11	0,09	100,3	377	180	49	70
0,695	0,05	0,3	99,32	263	420	49	120
0,726	0,05	0,63	99,8	282	360	47	120
0,619	0,05	0,78	99,79	213	360	54	200

Cu	Zn	Ga	Rb	Sr	Y	Zr	Nb	Cs
40	80	16	< 1	60	23,4	22	1,2	< 0,1
150	110	18	14	139	24,3	37	2	1
200	90	10	2	159	12,7	60	7,1	0,3
20	70	15	< 1	81	17,6	26	1,5	< 0,1
180	90	6	12	222	9,3	28	2,5	1,1
170	80	6	328	18	7,6	14	4,2	141
90	90	8	2	39	10,9	34	1,6	0,1
260	100	12	3	110	16,7	37	1,9	0,7
20	60	20	5	398	8,8	123	3,1	< 0,1
10	110	21	6	109	39,5	71	2	0,2
190	70	18	4	93	24,1	59	2	0,2
100	100	10	2	61	13,8	37	1,3	0,5
90	90	5	< 1	107	7,3	20	1,2	0,1
270	140	17	2	165	26,2	66	3,8	0,2
50	70	16	2	92	16,9	37	1,7	0,2
10	100	21	3	349	21,6	116	5,2	0,1
40	90	17	2	73	17,8	22	0,8	0,1
620	220	24	31	128	31,4	81	3,4	3,4
180	130	18	1	106	20,4	51	2,7	< 0,1
90	100	11	1	60	16,1	43	1,9	< 0,1
10	80	12	10	54	9,6	18	0,5	0,7
60	110	7	3	83	9,4	26	1,5	< 0,1
110	90	7	3	175	6,6	21	1,1	0,3
80	70	14	6	122	14,5	28	0,6	0,8
50	120	18	< 1	147	22,1	34	3,1	< 0,1
200	150	17	1	179	26,8	70	3,8	< 0,1
120	90	6	2	145	7,6	29	1,3	< 0,1
70	160	22	3	86	33,4	89	4,1	< 0,1
90	70	14	4	87	18	44	1,6	< 0,1
< 10	150	27	4	282	25,6	199	7,3	5,6
120	250	7	3	41	9	32	1,6	0,2
200	110	17	16	206	23,8	73	5,8	0,5
90	130	8	42	58	12,1	38	1,9	53,8
130	130	5	1	98	8,3	23	1,2	1
100	90	13	4	105	12,8	34	1,3	2,7
< 10	70	8	126	13	8	13	0,3	37,3
100	90	14	17	209	18,8	56	2,6	1
70	80	13	3	104	18	39	1,3	0,6
70	100	19	11	98	27,5	73	2,8	0,5
90	90	19	1	220	23,5	88	4,1	< 0,1
< 10	60	11	< 1	88	18,4	40	1,3	< 0,1
70	100	6	4	48	8,6	29	1,1	11,3
300	120	18	< 1	117	25,9	109	4,6	1,8
100	90	6	< 1	75	7,2	27	1	1,3
< 10	110	20	102	374	14,3	118	3,2	5,4
10	100	7	73	10	10,1	18	0,5	3,5
20	120	22	2	48	38	100	3,5	0,2
90	100	22	23	122	31,5	94	4,3	1,1
50	70	10	16	144	7,8	55	2,1	0,4
< 10	100	17	5	82	17,4	38	2,5	0,2
50	70	8	3	40	9,8	24	0,9	0,1
30	140	17	2	70	23,3	39	1,7	< 0,1
50	110	19	36	650	17,5	78	9,3	0,7
80	80	16	4	146	16,3	41	1,8	< 0,1
10	100	4	< 1	37	5,5	20	0,9	< 0,1
< 10	80	13	3	82	16,1	30	1,3	< 0,1

30	170	16	16	80	16,5	33	0,8	0,4
110	110	18	1	78	29,3	64	2,8	< 0,1
80	110	15	7	107	17,2	31	1,8	< 0,1
120	80	15	6	72	18	32	1,4	< 0,1
10	100	16	4	119	14	35	1,4	< 0,1

Ba	La	Ce	Pr	Nd	Sm	Eu	Gd	Tb
5	1,37	4,3	0,74	4,47	1,66	0,672	2,39	0,56
65	3,11	7,78	1,27	6,81	2,12	0,839	2,92	0,58
81	9,24	22,8	3,19	14,4	3,25	0,865	3,09	0,52
16	3,1	8,3	1,16	5,62	1,61	0,626	2,08	0,44
19	3,64	8,04	1,09	5,19	1,46	0,955	1,54	0,28
12	1,66	4,83	0,77	4,2	1,29	0,344	1,41	0,26
4	3,08	7,99	1,17	5,91	1,72	0,567	1,96	0,34
66	3,88	10,1	1,52	7,74	2,3	0,845	2,65	0,51
70	14,4	30,6	3,85	15,9	2,87	1	2,26	0,33
18	2,83	8	1,26	7,63	2,79	1,08	4,16	0,93
53	4,09	9,44	1,34	6,95	2,16	0,949	2,89	0,62
19	3,79	9,41	1,37	6,52	1,94	0,741	2,33	0,43
< 3	1,88	5,43	0,82	4,03	1,23	0,486	1,37	0,23
103	7,15	19,8	2,9	14,6	4,28	1,5	4,71	0,86
45	3,4	8,66	1,22	5,86	1,74	0,651	2,22	0,44
164	13,8	31	4,15	18,1	4,02	1,38	3,93	0,68
9	1,88	4,87	0,75	4,14	1,33	0,552	2	0,41
126	8,35	19,3	2,62	12,8	3,89	1,59	4,59	0,91
66	5,79	13,8	2,06	10,4	3,06	1,04	3,6	0,66
11	4,04	11	1,63	8,18	2,47	0,898	2,81	0,52
14	1,46	3,54	0,51	2,73	0,87	0,36	1,15	0,24
17	6,16	13,4	1,59	6,57	1,64	0,493	1,7	0,32
5	2,93	6,23	0,86	3,91	1,11	0,408	1,19	0,21
37	1,86	5,5	0,83	4,33	1,33	0,554	1,66	0,35
6	2,73	9,63	1,65	9,19	2,87	1,14	3,34	0,64
111	6	18	2,78	14,3	4,25	1,44	4,69	0,85
10	2,5	6,96	0,95	4,53	1,28	0,309	1,45	0,26
64	6,11	16,7	2,45	12,5	3,86	1,43	4,66	0,89
21	2,7	7,37	1,09	5,87	1,88	0,744	2,44	0,48
27	23	48,1	5,51	21,5	4,58	1,4	4,3	0,76
17	1,79	5,06	0,83	4,59	1,45	0,433	1,64	0,29
213	11,5	25,8	3,24	13,9	3,2	1,21	3,47	0,65
71	2,53	7,06	1,09	5,67	1,79	0,698	2,21	0,39
4	2,46	5,78	0,91	4,53	1,39	0,533	1,6	0,28
20	2,57	6,65	0,97	4,69	1,42	0,564	1,94	0,37
112	0,74	1,98	0,3	1,71	0,56	0,242	0,87	0,2
136	10,1	17,1	2,41	10,4	2,69	1,01	3,2	0,58
39	3,1	6,48	0,96	5,09	1,58	0,601	2,21	0,44
86	4,62	12,2	1,82	9,42	2,98	1,2	3,99	0,78
48	7,52	19,1	2,74	12,9	3,64	1,36	4,24	0,79
32	2,29	5,61	0,87	4,72	1,52	0,516	2,15	0,45
9	1,72	4,66	0,72	3,76	1,2	0,498	1,44	0,27
14	7,37	19,6	2,7	13	3,76	1,22	4,32	0,79
4	2,33	5,6	0,79	3,82	1,06	0,352	1,26	0,23
527	27,5	54,9	6,15	22,8	3,92	1,2	3,11	0,46
40	2,08	6,01	0,89	4,88	1,4	0,368	1,65	0,33
38	2,89	10,2	1,83	11,3	4,13	1,31	5,04	1,01
308	5,21	12,5	1,66	7,85	2,37	1,42	3,95	0,88
201	9,17	19,3	2,25	8,5	1,79	0,556	1,51	0,25
80	2,55	6,78	1,03	5,25	1,66	0,776	2,2	0,43
26	1,36	3,54	0,51	2,6	0,83	0,439	1,14	0,25
45	2,33	7,03	1,14	6,33	2,08	0,849	2,8	0,58
613	27,7	55,3	6,07	22,4	4,09	1,51	4,04	0,67
19	2,79	7,14	1,04	5,38	1,7	0,7	2,19	0,43
4	2,7	6,49	0,76	3,09	0,85	0,276	0,91	0,17
45	5,08	12	1,48	6,07	1,65	0,568	2	0,4

18	1,51	3,91	0,57	3,3	1,22	0,555	1,69	0,39
24	4,29	12,2	1,83	9,53	3,05	1,13	3,93	0,81
42	2,46	6,35	0,94	4,94	1,55	0,648	2,18	0,43
41	2,72	6,27	0,92	4,91	1,56	0,657	2,2	0,43
18	2,5	6,12	0,85	4,46	1,41	0,61	1,79	0,36

Dy	Ho	Er	Tm	Yb	Lu	Hf	Ta	W
3,9	0,83	2,57	0,409	2,64	0,408	0,9	0,06	< 0.5
3,96	0,84	2,57	0,386	2,47	0,379	1,3	0,12	< 0.5
2,81	0,51	1,38	0,188	1,11	0,163	1,8	0,6	< 0.5
2,96	0,62	1,91	0,295	1,93	0,295	1	0,14	< 0.5
1,7	0,32	0,85	0,119	0,73	0,111	0,8	0,59	< 0.5
1,53	0,29	0,78	0,109	0,67	0,099	0,5	6,71	< 0.5
2,09	0,4	1,13	0,159	1	0,147	1	0,13	< 0.5
3,16	0,61	1,74	0,251	1,59	0,242	1,2	0,13	< 0.5
1,72	0,31	0,85	0,121	0,78	0,118	3,1	0,17	< 0.5
6,46	1,4	4,34	0,658	4,29	0,656	2,2	0,13	< 0.5
4,12	0,85	2,58	0,393	2,62	0,401	1,8	0,14	< 0.5
2,68	0,52	1,46	0,211	1,31	0,201	1,1	0,11	< 0.5
1,36	0,26	0,75	0,108	0,66	0,094	0,6	0,08	< 0.5
5,27	1,01	2,84	0,394	2,41	0,361	2,2	0,29	< 0.5
2,9	0,6	1,79	0,277	1,82	0,278	1,1	0,12	< 0.5
3,98	0,78	2,26	0,333	2,19	0,342	3	0,36	0,6
2,91	0,64	1,95	0,3	2,02	0,313	0,8	0,04	< 0.5
5,69	1,1	3,27	0,494	3,09	0,474	2,4	0,79	80,8
4,1	0,78	2,23	0,317	1,98	0,297	1,5	0,2	0,8
3,19	0,61	1,73	0,247	1,52	0,231	1,4	0,14	< 0.5
1,63	0,35	1,06	0,161	1,07	0,165	0,6	0,05	< 0.5
1,91	0,35	1	0,14	0,88	0,13	0,8	0,13	< 0.5
1,27	0,24	0,67	0,096	0,6	0,09	0,5	0,08	< 0.5
2,44	0,53	1,6	0,242	1,61	0,268	0,8	0,03	< 0.5
4,04	0,79	2,34	0,347	2,17	0,337	1,2	1,11	< 0.5
5,25	1	2,8	0,396	2,42	0,37	2,2	0,27	< 0.5
1,51	0,28	0,77	0,109	0,68	0,104	0,8	0,1	< 0.5
5,77	1,19	3,58	0,538	3,46	0,509	2,4	0,29	< 0.5
3,22	0,67	2,04	0,303	1,97	0,308	1,3	0,12	< 0.5
4,65	0,93	2,78	0,431	2,78	0,411	5,1	0,81	1,2
1,8	0,35	0,98	0,141	0,86	0,123	0,9	0,13	< 0.5
4,11	0,84	2,53	0,375	2,42	0,373	2	0,43	< 0.5
2,41	0,46	1,3	0,189	1,16	0,161	1,1	0,14	< 0.5
1,67	0,31	0,87	0,124	0,75	0,11	0,6	0,09	< 0.5
2,43	0,5	1,47	0,217	1,38	0,21	1	0,09	< 0.5
1,39	0,3	0,92	0,136	0,84	0,12	0,4	0,01	< 0.5
3,59	0,7	1,99	0,285	1,79	0,28	1,7	0,22	< 0.5
2,98	0,64	1,93	0,29	1,88	0,298	1,1	0,14	< 0.5
5,12	1,03	3,13	0,475	3,03	0,449	2,2	0,21	< 0.5
4,73	0,9	2,57	0,382	2,4	0,356	2,6	0,34	< 0.5
3,04	0,65	2,02	0,312	2,08	0,314	1,2	0,09	< 0.5
1,68	0,31	0,84	0,116	0,7	0,105	0,8	0,09	< 0.5
4,8	0,92	2,61	0,371	2,33	0,334	2,9	0,38	< 0.5
1,35	0,25	0,73	0,11	0,7	0,106	0,8	0,08	< 0.5
2,58	0,48	1,36	0,203	1,3	0,188	3,1	0,27	0,7
2,05	0,37	1,03	0,149	0,91	0,125	0,6	0,04	< 0.5
6,64	1,31	4,01	0,627	4,17	0,626	2,9	0,26	0,6
5,82	1,13	3,41	0,531	3,44	0,526	2,8	0,41	0,9
1,5	0,29	0,83	0,122	0,76	0,111	1,4	0,15	< 0.5
2,89	0,6	1,77	0,27	1,78	0,263	1,1	0,1	< 0.5
1,73	0,36	1,07	0,159	1,03	0,159	0,7	0,06	< 0.5
3,87	0,79	2,37	0,365	2,39	0,355	1,2	0,06	< 0.5
3,66	0,65	1,75	0,238	1,44	0,202	2,4	0,52	1
2,86	0,58	1,7	0,248	1,58	0,232	1,2	0,25	< 0.5
1,06	0,19	0,56	0,088	0,57	0,08	0,5	0,06	< 0.5
2,65	0,56	1,75	0,278	1,84	0,282	0,9	0,1	< 0.5

2,71	0,59	1,8	0,28	1,9	0,299	1	0,06	< 0,5
5,38	1,1	3,33	0,526	3,43	0,496	1,9	0,19	< 0,5
2,89	0,61	1,84	0,276	1,8	0,275	1	0,1	< 0,5
2,89	0,61	1,87	0,284	1,87	0,285	1	0,08	0,6
2,44	0,5	1,48	0,223	1,45	0,219	1	0,1	< 0,5

Tl	Pb	Bi	Th	U
< 0,05	< 5	< 0,1	< 0,05	0,04
0,06	< 5	< 0,1	< 0,05	0,36
< 0,05	< 5	< 0,1	0,88	0,23
< 0,05	< 5	< 0,1	< 0,05	0,01
0,08	< 5	3,4	0,47	0,3
2,72	< 5	0,5	0,18	0,12
< 0,05	< 5	0,3	0,47	0,25
< 0,05	< 5	0,1	0,07	0,04
< 0,05	6	0,2	0,22	0,23
0,05	< 5	0,1	0,24	0,1
< 0,05	< 5	0,1	0,3	0,09
< 0,05	< 5	0,3	0,15	0,05
< 0,05	< 5	0,5	0,2	0,06
< 0,05	< 5	0,1	0,14	0,65
< 0,05	< 5	0,1	0,29	0,08
< 0,05	< 5	< 0,1	0,17	0,12
< 0,05	< 5	< 0,1	< 0,05	0,04
0,26	< 5	5,9	1,08	0,89
< 0,05	< 5	0,1	0,16	0,09
< 0,05	< 5	0,2	0,07	0,05
0,1	< 5	< 0,1	0,14	0,07
< 0,05	< 5	0,2	0,41	0,31
< 0,05	< 5	0,3	0,2	0,08
< 0,05	< 5	< 0,1	0,31	0,2
< 0,05	< 5	< 0,1	< 0,05	0,05
< 0,05	< 5	0,1	< 0,05	0,24
0,08	6	2	0,37	0,13
0,07	< 5	0,6	0,09	0,04
0,07	< 5	0,5	0,2	0,07
0,12	8	3,6	5	1,05
< 0,05	< 5	0,4	0,44	0,12
0,09	< 5	0,1	1,43	0,28
0,38	< 5	0,9	0,32	0,09
< 0,05	< 5	1,7	0,23	0,12
< 0,05	< 5	0,2	0,24	0,06
1	< 5	0,2	0,09	0,05
0,15	< 5	0,1	0,8	0,2
< 0,05	< 5	< 0,1	0,25	0,06
0,08	< 5	0,3	0,43	0,1
< 0,05	< 5	< 0,1	0,81	0,2
< 0,05	< 5	< 0,1	0,25	0,03
< 0,05	< 5	0,2	0,23	0,1
< 0,05	< 5	0,3	1,05	0,24
< 0,05	< 5	0,5	0,25	0,07
0,62	15	< 0,1	8,42	1,39
0,81	< 5	< 0,1	0,26	0,1
< 0,05	< 5	< 0,1	0,34	0,41
0,31	< 5	< 0,1	0,22	0,23
0,1	< 5	< 0,1	1,41	0,28
0,06	< 5	0,2	0,41	0,35
0,06	< 5	< 0,1	0,21	0,1
< 0,05	< 5	0,1	0,06	0,05
0,16	< 5	< 0,1	0,9	0,17
< 0,05	< 5	< 0,1	0,25	0,08
< 0,05	< 5	0,2	0,55	0,15
< 0,05	< 5	0,1	0,14	0,05

0,07	11	0,5	0,15	0,06
< 0,05	< 5	< 0,1	0,11	0,05
0,09	5	0,1	0,16	0,13
0,06	< 5	0,2	0,18	0,15
0,05	7	0,1	0,27	0,12